

Fire in ice: Two millennia of boreal forest fire history from the Greenland NEEM ice core

Piero Zennaro^{1,2,}, Natalie Kehrwald¹, Joseph R. McConnell³, Simon Schüpbach^{1,4}, Olivia J. Maselli³, Jennifer Marlon⁵, Paul Vallelonga^{6,7}, Daiana Leuenberger⁴, Roberta Zangrando², Andrea Spolaor¹, Matteo Borrotti^{1,8}, Elena Barbaro¹, Andrea Gambaro^{1,2}, Carlo Barbante^{1,2,9}*

* email: piero@unive.it phone number: +39 041 2348911 fax number: +39 041 2348549

¹ Ca' Foscari University of Venice, Department of Environmental Science, Informatics and Statistics, Santa Marta - Dorsoduro 2137, 30123 Venice, Italy.

² Institute for the Dynamics of Environmental Processes, IDPA-CNR, Dorsoduro 2137, 30123 Venice, Italy.

³ Desert Research Institute, Department of Hydrologic Sciences, 2215 Raggio Parkway, Reno, NV 89512 USA.

⁴ Climate and Environmental Physics, Physics Institute and Oeschger Centre for Climate Change Research, University of Bern, Sidlerstrasse 5, CH-3012 Bern, Switzerland

⁵ Yale University, School of Forestry and Environmental Studies, 195 Prospect Street, New Haven, CT 06511 USA.

⁶ Centre for Ice and Climate, Niels Bohr Institute, University of Copenhagen, Juliane Maries Vej 30, Copenhagen Ø, 2100 Denmark.

⁷ Department of Imaging and Applied Physics, Curtin University, Kent St, Bentley WA 6102, Australia.

⁸ European Centre for Living Technology, San Marco 2940, 30124 Venice, Italy.

⁹ Centro B. Segre, Accademia Nazionale dei Lincei, 00165 Rome, Italy

Abstract

Biomass burning is a major source of greenhouse gases and influences regional to global climate. Pre-industrial fire-history records from black carbon, charcoal and other proxies provide baseline estimates of biomass burning at local to global scales, but there remains a need for fire proxies that span millennia in order to understand the role of fire in the carbon cycle and climate system. We use the boreal fire biomarker levoglucosan, and multi-fire source black carbon and ammonium concentrations to reconstruct fire activity from the North Greenland Eemian (NEEM) ice cores (77.49° N; 51.2° W, 2480 masl) over the past 2000 years to infer changes in boreal fire activity. Increases in boreal fire activity over the periods 1000 - 1300 CE and 1500 - 1700 CE coincide with the most extensive central and northern Asian droughts of the past two millennia. Changes in the concentrations of biomass burning tracers in the NEEM ice cores coincide with temperature changes throughout much of the past 2000 years except for during periods of extreme drought, when precipitation changes are the dominant factor. Many of these multi-annual droughts are caused by Asian monsoon failures, thus suggesting a connection between low and high latitude climate processes. North America is a primary source of biomass burning aerosols due to its relative proximity to the NEEM camp. During major fire events, however, isotopic analyses of dust, back-trajectories and links with levoglucosan peaks and regional drought reconstructions suggest that Siberia is also an important source of pyrogenic aerosols to Greenland.

1. Introduction

1 Fire influences regional and global climate through the emission of greenhouse gases and particulates that reflect
2 and absorb incoming solar radiation (Ramanathan and Carmichael, 2008; Bowman et al., 2009; IPCC, 2013).
3 Biomass burning plays an important role in the carbon cycle as it emits up to 50% as much CO₂ as fossil fuel
4 combustion (Bowman et al., 2009). Fire products such as black carbon (BC) have a radiative absorption forcing
5 up to 55% that of CO₂, which is greater and a greater influence than that of other greenhouse gases, forcings
6 such as methane (CH₄), chlorofluorocarbons, nitrous oxide and tropospheric ozone (Ramanathan and
7 Carmichael, 2008; Jacobson, 2004; van der Werf et al., 2004; Running, 2006; McConnell et al., 2007).
8 Combined direct and indirect effects rank BC as the second-largest contributor to globally averaged positive
9 radiative forcing since the pre-industrial period (Ramanathan and Carmichael, 2008; Randerson et al., 2006).
10 Estimates of the radiative forcing of combined biomass burning aerosols are still not well defined but are in the
11 range of $+0.00 \pm 0.20 \text{ W m}^{-2}$ (IPCC, 2013). Human activities may have changed the net negative radiative
12 forcing of pre-industrial fires (-1.0 W m^{-2}) to approximately -0.5 W m^{-2} (from 1850 to 2000 CE) and potentially
13 to -0.8 W m^{-2} (from 1850 to 2100 CE) (Ward et al., 2012).

14
15 Fire influences the climate system, but in turn centennial-scale Holocene fire variations are influenced by climate
16 (Marlon et al., 2013; Power et al., 2008). Precipitation decreases fuel flammability (Pechony and Shindell, 2010)
17 but biomass burning is highest at intermediate moisture levels (Daniau et al., 2012), a balance must therefore be
18 struck between climatic conditions that are wet enough to allow biomass to grow, but dry enough to allow
19 combustion (Pyne, 2001). Increased temperatures and atmospheric CO₂ permit greater plant productivity and
20 could result in greater fuel availability and hence increased fire activity (Marlon et al., 2008; Daniau et al.,
21 2010). Human activities have also had an influence on biomass burning trends (Marlon et al., 2008) through
22 deforestation and slash-and-burn agricultural practices (FAO, 2007); practices which may have affected fire
23 regimes during the entire past millennia (Bowman et al., 2009; Kaplan et al., 2011; Ruddiman, 2003). The
24 observable impact of humans on fire regimes differs by geographic region (McWethy et al., 2009; Marlon et al.,

25 2012; Power et al., 2008) but over the course of the 20th century human activity has begun to influence the global
26 fire regime more than natural causes (Marlon et al., 2008; Pechony and Shindell, 2010).

27

28 1.1 *Boreal Forest Fires*

29 The circumpolar boreal zone contains about 30% of world's forests with half of the world's forest carbon and
30 about 30% of world's terrestrial carbon. Any change to the boreal forest carbon balance may therefore
31 considerably affect the global atmospheric CO₂ (Conard et al., 2002). Annual area burned (extent) and the global
32 importance of fires in the boreal zone have often been underestimated (Conard et al., 2002). However, it is
33 estimated that between 50,000 and 200,000 km² of boreal forests burn every year, mainly in Northern Asia and
34 North America (de Groot et al., 2013; Wooster and Zhang, 2004). On average boreal and temperate vegetation
35 fires represent 4% of global biomass burning and up to 12% during extreme events, when about 20% of global
36 BC may be produced (Lavoue et al., 2000). Thus, boreal forest fires are an important source of air pollutants
37 throughout the Arctic, and a major font of BC (Quinn et al., 2008; Lavoue et al., 2000). Due to the light-
38 absorbing properties of BC and the associated decrease in surface snow albedo, boreal forest fire BC has a
39 significant radiative impact on the Arctic atmosphere (Quinn et al., 2008; Flanner et al., 2007; Hansen and
40 Nazarenko, 2004).

41

42 North American and Eurasian boreal fire regimes differ due to distinctive fuel, weather, and fire ecology
43 (Wooster and Zhang, 2004; de Groot et al., 2013). Mean fire intensity and fuel consumption is higher in North
44 America than in Russia, even though the spatial extent of forests is greater in Russia (Wooster and Zhang, 2004;
45 de Groot et al., 2013). Different fire regimes suggest a dominance of crown fires in North America and surface
46 fires in Russia (Wooster and Zhang, 2004; de Groot et al., 2013). Accordingly, Russian fires may burn less fuel
47 than North American fires (de Groot et al., 2013) and thus emit less pyro-products into the atmosphere per unit
48 of area burned (Wooster and Zhang, 2004). Over the period 2001-2007, the average size of large fires in Central
49 Siberia was estimated as approximately 13.1 km², with an average 18,900 km² burned each year at an average
50 fire intensity of 4858 kW m⁻¹ (de Groot et al., 2013). In western Canada the annual average size of individual

51 large fires is 59.3 km², with a total of 5,600 km² burned annually and an average fire intensity of 6047 kW m⁻¹
52 (de Groot et al., 2013). The carbon emission rate is 53% higher in the Canadian study area, due to higher pre-
53 burn forest floor fuel loads and higher fuel consumption by crown fires. However, the Russian study area had
54 much higher total carbon emissions due to the greater annual area burned (de Groot et al., 2013). During the
55 major fire year of 2004, an additional 31,000 km² of Canadian boreal forests and approximately 27,000 km² of
56 Alaskan forests burned (Stohl et al., 2006) resulting in strong Pan-Arctic enhancements of light absorbing
57 aerosols (Stohl et al., 2006). This strong burning year in Canada and Alaska is coincident with a pronounced
58 decrease in snow albedo at Summit, Greenland due to the deposition of dark particles on the snow surface.
59 Boreal forest fires in Siberia may have a larger impact on total global fire emissions than those in North America
60 due to the larger Siberian burn area (Stohl, 2006; Stohl et al., 2006). Siberian forest fires are a major
61 extratropical source of carbon, in particular carbon monoxide and black carbon (Lavoue et al., 2000). Russian
62 boreal forests, where the majority are located in Siberia, accounted for 14–20% of average annual global carbon
63 emissions from forest fires in 1998 (Conard et al., 2002). However, little is known about the emission, transport
64 and deposition of BC from Siberian forest fires to the Arctic. The characterization of Siberian fire plumes is
65 uncertain, due to currently undefined biomass fraction consumed, combustion efficiency, plume injection heights
66 and emission ratios (Paris et al., 2009). Models are sensitive to the conditions and types of fires, such as the
67 injection height of fire emissions (Turquety et al., 2007), and the lack of data about Siberian fires introduces
68 large potential errors in estimating the impact of boreal wildfires on the atmospheric composition (Conard et al.,
69 2002).

70

71 Summer atmospheric conditions favour enhanced wet and dry BC deposition in the Arctic (Stohl, 2006).
72 Generoso et al. (2007) determined that the 2003 Russian fires contributed to approximately 40–56% of the total
73 BC mass deposited north of 75 °N. In fact, model results indicate that boreal forest fire sources, especially
74 Siberian fires, are the dominate summer-time source of BC reaching the Arctic, exceeding all contributions from
75 anthropogenic sources (Stohl, 2006). Siberian fires, and northern Eurasia sources in general, can reach the Arctic
76 more easily than emissions from other regions of similar latitude (Stohl, 2006; Stohl et al., 2006).

77

78 *1.2 Biomass Burning Proxies*

79 There are many potential indicators or proxies of past fire activity, such as altered products of plant combustion
80 (e.g. charcoal, BC), partially combusted biological material (e.g. fire scars in tree rings), or chemical markers
81 directly produced and volatilised during vegetation combustion (e.g. resin acids, polycyclic aromatic
82 hydrocarbons) (Conedera et al., 2009). Some proxies are specific as they are produced solely from biomass
83 burning, such as charcoal in sediment cores, but most others have multiple potential sources other than wildfires
84 (e.g., coal burning, volcanic eruptions or biogenic emissions). Ice cores from polar regions are widely used to
85 reconstruct detailed climate records over the past hundreds of thousands of years, and thus are powerful tools in
86 paleoclimate research. Examining forest fires in ice cores started with the pioneering work of Legrand et al.
87 (1992), which demonstrates that the concentration of ammonium and organic acids including light carboxylic
88 acids, significantly increase above background levels in Greenland ice layers during forest fire events. Among
89 possible light carboxylic acids, formate and oxalate are the most useful to trace fires in Greenland ice cores
90 (Jaffrezo et al., 1998; Legrand et al., 1992; Dibb et al., 1996; Kehrwald et al., 2012). The subsequent work of
91 Legrand and DeAngelis (1996) demonstrates that high latitude biomass burning episodes increase light weight
92 carboxylic acid concentrations by 20 – 30 % in Greenland ice. In addition to strong increases of ammonium,
93 formate and oxalate concentrations, Savarino and Legrand (1998) found slight increases of nitrate coincident
94 with fire events recorded in Greenland ice. However, lightweight carboxylic acids and major ions (potassium
95 (K^+), ammonium (NH_4^+) and nitrate (NO_3^-)) are not specific for biomass burning since they can be emitted by
96 multiple sources. K^+ and NH_4^+ , for example, are also emitted from numerous other sources and thus must be
97 corrected accordingly in order to provide source-specific information (Savarino and Legrand, 1998). Of the
98 available ionic proxies, K^+ is less useful due to marine and terrestrial sources, even if corrected to remove these
99 contributions (e.g. non-sea-salt and non-crustal K^+) (Legrand and DeAngelis, 1996; Savarino and Legrand, 1998)
100 Statistical attempts to recognize forest fire signals from multiple ice core data sets use Empirical Orthogonal
101 Function (EOF) analysis or Principal Component Analysis (PCA), which identify chemical associations between
102 pyro-ion records and differentiate between sources and transport characteristics (Yalcin et al., 2006; Eichler et

103 al., 2011). NH_4^+ , NO_3^- , and organic acids in Greenland ice are often associated with biomass burning events,
104 where NO_3^- in particular tends to increase in samples with higher NH_4^+ concentrations (Fuhrer et al., 1996;
105 Whitlow et al., 1994; Savarino and Legrand, 1998). These indicators are a result of complex chemical reactions
106 that are not necessarily a direct reflection of variations in biomass burning, however, many high fire years are
107 identifiable by enhanced NH_4^+ concentration (Eichler et al., 2011).

108 The isotopic ratio of atmospheric gases, such as methane (CH_4) and carbon monoxide (CO) in Antarctic (Ferretti
109 et al., 2005; Wang et al., 2010) and Arctic (Sapart et al., 2012) ice cores has also been used as fire proxy but
110 such ratios are also not solely products of biomass burning (Fischer et al., 2008). The isotopic composition of
111 methane ($\delta^{13}\text{C}$ of CH_4) in ice cores differentiates biogenic from pyrogenic sources (Sapart et al., 2012). Methane
112 is stable in the atmosphere for longer than the atmospheric exchange time and therefore is globally distributed.
113 Hence $\delta^{13}\text{C}$ of CH_4 variations are impacted by sources distributed all over the world (Blunier et al., 2007).

114

115 BC is emitted during incomplete combustion of fossil and biofuels in both naturally and anthropogenically
116 created fires (Preston and Schmidt, 2006; McConnell et al., 2007). BC is not a single chemical compound,
117 however, and lacks well-defined characteristics (Goldberg, 1985; Masiello, 2004). However, comparison BC
118 with vanillic acid, a lignin phenol tracer of conifer combustion (Simoneit, 2002), in an ice core from west central
119 Greenland allowed McConnell (2007) to separate out the contributions of biomass burning and fossil fuels to the
120 BC flux reaching Greenland. Other specific tracers for biomass burning, including levoglucosan (vegetation
121 fires) and p-hydroxybenzoic and dehydroabiatic acids (conifer fires), have been analyzed in high and mid-
122 latitude ice cores from the Kamchatka Peninsula, Northeast Asia (Kawamura et al., 2012) and from the Tibetan
123 Plateau (Yao et al., 2013).

124

125 Monosaccharide anhydrides are one of the few fire proxies that have specific sources (Gambaro et al., 2008;
126 Simoneit, 2002). Levoglucosan (1,6-anhydro- β -D-glucopyranose) is a monosaccharide anhydride released
127 during biomass burning when cellulose combustion occurs at temperatures $>300^\circ\text{C}$ (Gambaro et al., 2008;
128 Simoneit, 2002). As with BC and NH_4^+ , levoglucosan is injected into the atmosphere in convective smoke

129 plumes, deposited on glacier surfaces through wet and dry deposition, and preserved in the snow and ice
130 (Gambaro et al., 2008; Kehrwald et al., 2012; McConnell et al., 2007; Fuhrer and Legrand, 1997). Unlike
131 greenhouse gases, levoglucosan, NH_4^+ and BC are not homogeneously distributed in the atmosphere as chemical
132 processing causes short lifetimes (on the order of days to weeks) (Hennigan et al., 2010; Fraser and Lakshmanan,
133 2000; Ramanathan and Carmichael, 2008; Fuhrer and Legrand, 1997) in addition to efficient deposition
134 processes from the atmosphere. Although levoglucosan is oxidized by OH radicals in the gas phase (Hennigan et
135 al., 2010) and in atmospheric water droplets (Hoffmann et al., 2010), its high concentration in biomass emissions
136 means that levoglucosan remains a strong potential tracer for fire activity even across remote distances (Fraser
137 and Lakshmanan, 2000; Holmes and Petrucci, 2006, 2007; Kehrwald et al., 2012).

138

139 Charcoal deposited both in non-polar ice and sediment cores can also help reconstruct past fire activity. The
140 Global Charcoal Database (GCD) compiles individual charcoal records from terrestrial and marine sediment
141 cores (Fig. S6) into global or regional reconstructions that provide a benchmark against which other biomass
142 burning records can be compared (Power et al., 2010; Marlon et al., 2008). The charcoal database covers all
143 climatic zones and all major biomes, but data for grasslands and dry shrublands, where low woody biomass
144 limits charcoal production, are limited due to a lack of suitable sampling sites (Marlon et al., 2008). These
145 vegetation types emit large quantities of levoglucosan when burned (Iinuma et al., 2007; Gao et al., 2003)
146 resulting in a possible offset between charcoal and levoglucosan data. Many charcoal sampling sites are located
147 in the US and Europe, and a limited number of GCD sites currently exist in northern Asia (Fig. S6). As
148 levoglucosan and BC can be transported hundreds to thousands of kilometers (Mochida et al., 2010), they
149 complement GCD reconstructions that record combustion within tens of km of the sampling sites, and provide
150 fire activity data for regions where charcoal records do not exist.

151

152 *1.3 Aim of the Study*

153 Here, we use a multi-proxy approach to reconstructing biomass burning in the northern high latitudes during the
154 past 2000 years. Specifically, we report levoglucosan and ammonium concentrations in the upper part of the

155 deep North Greenland Eemian (NEEM) ice core as well as BC measured in the 410 m NEEM-2011-S1 core
156 (Fig. 1) which was collected adjacent to the deep core in 2011 (Sigl et al., 2013). We compare our results with
157 Northern Hemisphere fire records, climate conditions obtained from historical records and paleoarchives to
158 identify sources of and controls on fire emissions registered in NEEM. Our approach acknowledges the
159 weaknesses inherent in most fire proxies used in ice core studies and remedies this by integrating the results
160 from multiple fire proxies to identify the robust variations in past biomass burning during the past 2000 years.
161

162 **2. Methods**

163 *2.1 Ice core sampling and analyses*

164 The international North Greenland Eemian (NEEM) ice core drilling site (Fig. 1) is located in northwest
165 Greenland (77.49 N; 51.2° W, 2480 masl, mean annual temperature -29 °C, accumulation 0.22 m ice equivalent
166 yr⁻¹). The deep NEEM ice core (Fig. 1) was drilled from 2008 to 2012 and reached a depth of 2540 m. Ice core
167 analyses were partly performed in the field and partly in the laboratories of the participating nations. Our
168 levoglucosan dataset consists of 273 samples from 4.95-602.25 m depth (1999 CE - 1036 BCE), where each
169 sample is a 1.10 m inner core section collected after being melted within the Continuous Flow Analysis (CFA)
170 (Kaufmann et al., 2008) system at the NEEM camp. Samples for levoglucosan determination were transported in
171 a frozen state from the field to Ca' Foscari University of Venice laboratory where they were stored in a -20 °C
172 cold room until analysis. We slightly modified the analytical procedure for determining levoglucosan
173 (Supplementary Information) using liquid chromatography / negative ion electrospray ionization - tandem mass
174 spectrometry (HPLC/(-)ESI-MS/MS) at picogram per milliliter reported by Gambaro *et al.* (2008)
175 (Supplementary Information). This analytical method has the advantage of allowing the direct determination of
176 levoglucosan by introducing the melted sample and ¹³C₆ labeled internal standard into the HPLC instrument.
177 Preanalytical procedures (analyte extraction and purification) are avoided and sample contamination minimized.
178 NH₄⁺ and the other major ions were measured by CFA on the deep NEEM core directly in the field during
179 season 2009 (Kaufmann et al., 2008). All the major ions are available at mm resolution, and we calculated 1.1 m
180 mean values in order to directly compare with levoglucosan.

181

182 The upper 1419 m of deep NEEM core d¹⁸O, volcanic fingerprints, Electrical Conductivity Measurement,
183 Dielectrical Profiling, and impurity records can be matched to the NGRIP GICC05 extended time scale (Fig S7)
184 (Wolff et al., 2010b; Rasmussen et al., 2013). Due to the ice compression and differences in Greenland snow
185 accumulation, each 1.10 m sample covers 1 to 5 yr-long temporal periods. The temporal interval has an
186 associated age error of ±1 year from the top of the ice core to the depth of 294.25 m (698 CE) and from 338.25
187 m to 536.8 m (468 CE – 645 BCE). An error of ± 2 years exists from 295.35 m to 336.05 m depth (692 – 480

188 CE) and from 541.20 m to 602.25 m (671 - 1036 BCE). No official age model is currently available for the upper
189 section (0.00 – 19.80 m) of the NEEM ice core. The uppermost 20 m of the age scale was calculated using a
190 Herron-Langway firn densification model fit to the NEEM-NGRIP tie points for the 20-80 m long firn column
191 (Fig. S7) (Herron and Langway Jr, 1980).

192

193 Continuous flow analysis allows sub-seasonal reconstructions of BC in the NEEM-2001-S1 core (Sigl et al.,
194 2013) and other Greenland ice cores (McConnell et al., 2007; McConnell and Edwards, 2008; McConnell,
195 2010). The NEEM-2011-S1 core was collected adjacent to the deep NEEM core (Fig. 1) in summer 2011 and the
196 410 m long core was transported to the Desert Research Institute in Reno, NV, USA. The core was cut into ~1.1
197 m long samples with cross section of ~ 0.033 m by 0.033 m. These longitudinal samples were analyzed in early
198 autumn 2011 using a well-established continuous ice core analytical system (McConnell, 2002; Banta et al.,
199 2008) including determination of BC concentrations using methods described in McConnell et al. (2007) and
200 McConnell and Edwards (2008). Annual layer counting based on seasonal variations in a number of elements
201 and chemical species, constrained by the known volcanic markers in the deep NEEM and other ice cores, was
202 used to determine the age model with dating uncertainty of <1 year. (Sigl et al., 2013). BC was measured using a
203 continuous ice core melter system (McConnell and Edwards, 2008; McConnell et al., 2007) in the 410 m
204 NEEM-2011-S1 core collected adjacent to the deep NEEM core in 2011 (Fig. 1). We present 1921 BC
205 concentrations from the NEEM-2011-S1 cores, spanning the ages 78 - 1997 CE. A number of seasonally varying
206 elements and chemical species were used to count annual layers in the NEEM-2011-S1 core, resulting in
207 minimal dating uncertainty (Sigl et al., 2013) as for the deep NEEM core dating (Supplementary Information).

208

209 The BC and levoglucosan measurements were sampled at different resolutions. Because of the non-linearity of
210 the ice depth – ice age relationship this means that the average depth of samples measured at different resolution
211 will represent a NEEM-2011-S1 and deep NEEM ice cores have different sampling schemes, this difference
212 means that BC samples and levoglucosan samples represent similar, but not equal, average age of the ice. BC is
213 sampled at a higher resolution (sub-annual resolution) than the levoglucosan (one sample continuously covering

214 1.10 m of the deep NEEM ice core). In order to avoid temporal resolution loss and the introduction of errors, we
215 chose not to calculate BC averages from NEEM-2011-S1 core over the same temporal interval covered by the
216 deep NEEM core when seeking to compare pyro-proxies from the two cores, instead leaving them as annual BC
217 concentrations.

218

219 2.2 *Statistics*

220 One of the first challenges to understanding that levoglucosan reflects variations in fire activity is to assess its
221 relationship with transport variability. Dust and Ca^{2+} concentrations can be used as crustal particulate tracers in
222 ice cores, provide clues into the relative strength of their source regions, transport variability and transport
223 strength (Fischer et al., 2007; Obrien et al., 1995; Wolff et al., 2010a). The Holocene contribution of sea salts to
224 total Greenland Ca^{2+} ice concentrations is estimated to be in the order of 10% (Fischer et al., 2007). In order to
225 keep the data as close to its original form as possible, and therefore to avoid including possible error due to data
226 transformation, we use Ca^{2+} as a dust tracer without correcting for sea salt contribution. Then, we studied links
227 between levoglucosan, ammonium and major ions by performing Pearson and Spearman correlations
228 (Supplementary Information).

229

230 2.3 *Short- to long-term fire variation*

231 For short-term analysis, we consider *megafires* as levoglucosan peaks with a Z-score ≥ 1 [$Z\text{-score} = (x_i - \bar{x})/\sigma$],
232 corresponding to a concentration $\geq 245 \text{ pg mL}^{-1}$ (Table 1, Figure S5). Multi-decadal fire activity was
233 extracted from the levoglucosan and BC concentration profiles by analyzing smoothed data after removing
234 spikes above a fixed threshold (Supplementary Information). We tested different approaches in order to
235 determine multi-decadal fire activity from levoglucosan concentrations. The challenge was to find a suitable
236 statistical tool capable of identifying temporal trends that are not overly affected by the high peaks of anomalous
237 events. The Global Charcoal Database archives hundreds of sedimentary records of fire (Power et al., 2010).
238 Regional and global synthesis allows the examination of broad-scale patterns in paleofire activity (Marlon et al.,
239 2013). In order to compare levoglucosan data with decadal to centennial trends in other paleoclimate records, we

240 first applied the same standardized statistical procedures as was used to analyze the Global Charcoal Database
241 (Marlon et al., 2008; Power et al., 2008). We modified this method for the NEEM data as it is from a single site
242 (unlike the GCD) and incorporating any outlying values results in artifacts in the LOWESS smoothing. A
243 common approach to isolate the influence of spikes is to fix a threshold and separately study those values. We
244 differ from the GCD procedure in our treatment of individual spikes, as these strongly affect multi-decadal
245 trends, even when using a LOWESS regression model.

246 In summary, to highlight long-term fire changes we followed the following procedure (details are included in the
247 Supplementary Information):

- 248 • Removing spikes above the fixed threshold $3rd_Q + 1.5 \times IR$
- 249 • Z-score transformation
- 250 • LOWESS (Locally Weighted Scatterplot Smoothing) model

251

252 **3 Results**

253 Pearson and Spearman correlations (Supplementary Information) demonstrate that, of the possible biomass
254 burning-related products measured in the deep NEEM core, levoglucosan concentrations only slightly correlate
255 with ammonium (p-value $< 10^{-6}$, with $\alpha = 0.05$). No correlation is noted between levoglucosan and crustal
256 marker Ca^{2+} or dust (p-values > 0.45 , with $\alpha = 0.05$). Analysis of preliminary measurements of other crustal
257 markers (i.e. Ti and Ba) in the deep NEEM ice core also show a lack of correlation with levoglucosan (Gabrieli,
258 J., personal communication, 2014). A similar correlation analysis of BC and other elements and chemical species
259 (data not shown) measured in the NEEM-2011-S1 core indicates that during pre-industrial periods BC
260 concentrations generally do not correlate with crustal particulate tracers but do with NH_4^+ and NO_3^- (J.R.
261 McConnell, Personal Communication, 2014).

262

263 Megafires (levoglucosan peaks with Z-scores > 1) are observed at 1973, 1789, 1704, 1620, 1039, 976, 922, 628,
264 342 CE and at 199, 274, 330, 392 and 540 BCE (Fig. 2 and Table 1). Distinct levoglucosan spikes are also
265 synchronous with major peaks in the BC record (BC Z-scores > 3) at 1704, 922, 628 and 342 CE and minor
266 peaks (with BC Z-scores > 1) at 1973, 1789, 1620 and 976 CE, respectively. The levoglucosan peak at 342 CE
267 (Z-score = 10.9) also occurs in the BC data, where the Z-score is 19.0 (Table 1).

268

269 Strong fluctuations in the temporal profile dominate the record from decadal to centennial perspectives. Relative
270 maxima in the levoglucosan profile are evident between 1000 - 1300 CE and 1500 - 1700 CE, and with a lesser
271 extent around 500 CE and 100 CE, while the lowest fire activity is evident around 700 - 900 CE and with a
272 lesser extent around 1300 - 1500 and 1700 - 1800 CE (Fig. 3A). Smoothed BC concentration is high from 100
273 CE to 700 CE, and after an abrupt decrease it offers the lowest values between 700 CE and 900 CE. Between
274 1000 - 1600 CE and 1600 - 1800 CE the BC profile show a relative maximum and minimum, respectively, while
275 the absolute maximum in BC concentration peaks around 1900 CE.

276

277 **4 Discussion and Interpretation**

278 *4.1 Biomass burning tracers in the NEEM ice core*

279 *4.1.1 Major ions transport and deposition on the Greenland ice-sheet*

280 Dust, major ions and levoglucosan may not have the same source regions and/or transport history, but comparing
281 these proxies may provide insight into common or differing air masses affecting the NEEM site. Increased wind
282 speeds result in greater dust concentrations and larger particles in ice cores (Ruth et al., 2003; Fischer et al.,
283 2007). Stronger winds may be expected to also increase levoglucosan concentrations, as the increased wind
284 strength could transport more efficiently air plumes and thus more biomass burning products. However, the lack
285 of correlation between Ca^{2+} , dust and levoglucosan suggests that levoglucosan variability is not dominated by
286 changes in transport or in changes in wind strength. This evidence differs from Kawamura et al.'s (2012)
287 conclusion, which speculated that enhanced atmospheric transport rather than an increase in fire activity may
288 affect levoglucosan concentrations.

289

290 Ammonium has multiple anthropogenic and natural sources, mainly emissions from soil and vegetation and thus,
291 background ammonium values in polar ice are strongly linked to biogenic emissions and temperature changes
292 (Fuhrer et al., 1993; Fuhrer et al., 1996; Legrand et al., 1992; Fuhrer and Legrand, 1997). Basing NEEM fire
293 reconstructions only on ammonium concentrations that are not corrected for the natural variability and volcanic
294 eruptions could potentially overestimate major fire events, however, comparing various fire proxies from the
295 same core supplements biomass burning interpretations. The literature uses Principal Component Analysis for
296 pyro-reconstructions (Yalcin et al., 2006; Eichler et al., 2011). Incorporating as many fire proxies as possible
297 within the same ice core allows a more robust reconstruction of past burning, but eigenvectors incorporate other
298 chemical species that, even if they are fire-related compounds, are not fire tracers (NO_3^- , H_2O_2). We therefore
299 compare individual fire tracers in NEEM rather than using Principal Component Analysis as a biomass burning
300 reconstruction.

301

302 *4.1.2 Extreme fire events*

303 Levoglucosan data exhibit high variability (Fig. 2) due to the absence of background atmospheric levoglucosan
304 values. Levoglucosan is only injected into the atmosphere during biomass burning events; no continuous
305 emission processes exist. Individual levoglucosan spikes are therefore likely generated either by short
306 “megafires” or by localized fire events rather than by long-term increases in fire activity (Fig. 2 and S5 in the
307 Supplement). Furthermore, the mean accumulation rate in north central Greenland can be considered constant
308 over the past 3000 years (Andersen et al., 2006), so we present levoglucosan and BC concentrations rather than
309 fluxes.

310

311 Many levoglucosan spikes correspond with documented fire activity in Greenland or in other Northern
312 Hemisphere ice cores, and are generally supported by the other pyro-proxies measured in the NEEM ice core
313 (Table 1). The majority of fire events inferred from the NEEM ice core were simultaneously recorded by
314 levoglucosan and BC. NH_4^+ spikes replicate many of the levoglucosan spikes (8 of the 14 levoglucosan spikes
315 with Z-score >1). Only the 1039 CE levoglucosan peak is not duplicated by any of the other proxies (Table 1).
316 The peak at 342 CE contains by far the highest concentrations of both levoglucosan and BC present in our
317 datasets, and corresponds to the largest fire event in the past 2000 years recorded by several charcoal records in
318 the Northern U.S. and Canadian Rockies (Brunelle et al., 2005; Hallett et al., 2003). The 1973 CE fire event is
319 synchronous (within the age model error) and probably related to an anomalous heat wave and severe droughts
320 in 1972 CE in Russia (Dronin and Bellinger, 2005; Golubev and Dronin, 2004). Thousands of Russian firemen,
321 soldiers and farmers were mobilized to suppress a fire raging for several weeks in August 1972 in a bog-land
322 east of Moscow (The Palm Beach Post, Aug. 09 1972; The New York Times, Aug. 09 1972, New York), and
323 during the same week more than 1000 km² of forest burned in Central Alaska (The Milwaukee Journal, Aug. 09
324 1972).

325

326 We cannot exclude the possibility that local phenomena in Greenland, rather than extensive events, may be
327 responsible for some of the large levoglucosan spikes. Several levoglucosan spikes were recorded in a relatively
328 brief period between ~ 920 and 1110 CE. This period coincides with the foundation of Viking settlements in

329 Greenland beginning in 982 CE in southwest Greenland, relatively close to the NEEM site. Historical records
330 show that Greenland Viking settlements burned vast quantities of wood for extracting iron from bogs for tool
331 production and these local, not necessarily extensive, fires may account for the levoglucosan peaks during this
332 time period (Diamond, 2005). Future trace metal analyses of the NEEM ice core can help demonstrate if
333 relatively local metal production may have caused these levoglucosan peaks.

334

335 Other ice core records provide comparisons of fire events that allow an examination of the spatial extent of past
336 short-lived fire activity. A prominent 1617 - 1622 CE levoglucosan peak coincides with high fire activity
337 inferred from oxalic acid analyses recorded in the Greenland Site J ice core (Kawamura et al., 2001), even if this
338 event is not recorded in ice core from other locations in Greenland (e.g. Savarino and Legrand, 1998). No
339 historical documentation is available for the 1787 - 1791 CE peak but contemporaneous fire signatures are
340 reported in Greenland (GISP2, 20D) and Canadian ice cores (Eclipse Icefield and Mt. Logan) (Yalcin et al.,
341 2006; Whitlow et al., 1994). The strongest fire activity recorded in the Ushkovsky (Kamchatka) ice core occurs
342 in 1705, 1759, 1883, 1915, 1949 and 1972 CE (Kawamura et al., 2012). Megaevents are present as both
343 levoglucosan and BC peaks in NEEM in 1704 and 1973 CE and as a BC peak in 1914.5 and 1947.5 CE (Fig. 2).

344

345 *4.1.3 Decadal to centennial fire activity variability*

346 The NEEM levoglucosan centennial scale maximum (1500 - 1700 CE, Fig. 3A), the highest of the past two
347 millennia, coincides with data from the Belukha ice core, Siberia (Eichler et al., 2011), that documents a period
348 of increased fire activity between 1550 - 1700 CE where 1600 - 1680 CE records the highest forest fire activity
349 over the last 750 years (Fig. 3D). High fire activity between 1500 - 1600 CE was also inferred from formate and
350 ammonium analyses on the EUROCORE, Greenland ice core, when “high frequency and low intensity of fires”
351 were synchronous with dry climate conditions (Savarino and Legrand, 1998).

352

353 Due to multiple anthropogenic BC sources after the Industrial Revolution, we cannot directly compare BC and
354 levoglucosan after 1850 CE but we can compare BC between NEEM and other Arctic sites and use our data to

355 discriminate fire, volcanic or anthropogenic emissions. The maximum BC concentration (16 ng g^{-1}) in the entire
356 Greenland D4 ice core occurred in 1908 CE (McConnell et al., 2007). The second-highest BC peak (15 ng g^{-1})
357 over the past millennium in the NEEM-2011-S1 is dated to 1909.5 CE (Fig. 2B). This timing is relatively
358 coincident with the Tunguska Event, a bolide impact in western Siberia occurring in June 1908. An ammonium
359 spike in 1910 CE in the GISP2 ice core (Taylor et al., 1996) was attributed to large conflagrations in the northern
360 United States and southern Canada, supported by a synchronous extremely limited growth of regional trees
361 (drought proxy) in the Northwestern Ontario (St. George et al., 2009). The highest ammonium peak in a Summit,
362 Greenland ice core spanning 1908-1989 CE occurs in 1908 CE and is synchronous with increases in formate,
363 oxalate, glycolate and BC within the same core. Legrand et al. (1995) ascribe this event to North American
364 forest fires rather than the Tunguska event. However, ammonium may be produced by a Haber-like process
365 (Melott et al., 2010). High pressure and temperature conditions generated by the Tunguska comet entering the
366 atmosphere, in principle could have allowed atmospheric nitrogen and hydrogen from the comet ice to react,
367 thereby accounting for both the ammonium and nitrate enhancements in some Greenland ice cores (Melott et al.,
368 2010). The absence of levoglucosan and ammonium spikes in the NEEM (northern Greenland) ice core or
369 vanillic acid peaks, a source-specific tracer for conifers (Simoneit, 2002), in the D4 (central Greenland) ice core
370 during this same time period, supports the hypothesis that BC, NH_4^+ and NO_3^- peaks may not be caused by forest
371 fires during 1908 CE. In addition, comparisons of BC and toxic heavy metals in the ACT2 core from southern
372 Greenland (McConnell and Edwards, 2008), as well as BC and non-sea-salt sulfur in the D4 ice core from
373 central Greenland (McConnell et al., 2007), indicate that >80% of the BC during this period is associated with
374 industrial emissions (primarily coal burning). The D4 site demonstrates a gradual rise in BC concentrations after
375 1850 CE and a rapid increase after 1888 CE, before beginning a gradual decline through the late 1940s followed
376 by a clear drop in 1952 CE (McConnell et al., 2007). This trend is generally confirmed by BC in the NEEM-
377 2011-S1 ice core, where BC shows a peak that slowly increases from ~ 1750 CE, followed by a sharp
378 enhancement during the late 1800s (Fig. 3C).

379

380 Biomass burning was the major source of BC to central Greenland before 1850 CE, as revealed by the close

381 correlation between BC and vanillic acid, an organic combustion marker released by coniferous trees
382 (McConnell et al., 2007). After 1850 CE, the influence of industrial emissions, particularly coal, as a source of
383 BC is clear through comparisons to non-sea-salt sulfur (McConnell et al., 2007) and industrial heavy metals such
384 as lead, thallium, cadmium in the southern Greenland ACT2 core (McConnell and Edwards, 2008). The NEEM-
385 2011-S1 BC record contains its highest concentrations from 1850 CE to the present, reflecting the input of these
386 new sources.

387

388 The levoglucosan profile contains moderately high mean values during the 1900s, but other centennial-scale
389 peaks, such as that centered ~ 1600 CE have higher concentrations (Fig. 2A). Black carbon has an average
390 atmospheric lifetime of a few days to one week (Ramanathan and Carmichael, 2008; Bauer et al., 2013;
391 McConnell et al., 2007). The diverse range of BC emission sources and the different atmospheric lifetime of
392 levoglucosan may result in BC representing a separate emission source area than the levoglucosan record.
393 Levoglucosan yield is variable and strongly depends on combustion temperature, biomass composition and
394 flame conditions (Gao et al., 2003; Oros and Simoneit, 2001a, b; Weimer et al., 2008). Thus, levoglucosan can
395 not be used to characterize and quantify BC in environmental samples (Kuo et al., 2008). In addition, different
396 temporal resolution for BC and levoglucosan records may result in differences after removing spikes and
397 applying LOWESS smoothing. Levoglucosan can only be produced by cellulose pyrolysis, thus the different
398 pattern between the records post-1850 CE mainly reflects the differences between biomass burning and
399 industrial activity.

400

401 4.2 Comparison with other pyro-reconstructions

402 The high latitude northern hemisphere HLNH > 55° GCD composite curve registers a global long-term decline
403 in fire activity from 0 - 1750 CE (Marlon et al., 2008). A decreasing amount of ammonium originating from
404 biomass burning is also deposited in the GRIP ice core (Fuhrer et al., 1996) but this trend is not clearly supported
405 by levoglucosan data during the past two millennia (Fig. 3B). The prominent levoglucosan minimum between
406 700 and 900 CE coincides with a minimum in the BC profile and HLNH > 55° GCD (Fig. 3). The HLNH > 55°

407 GCD and levoglucosan data differ near 1600 CE when the HLNH > 55° GCD demonstrates a modest increase in
408 fire activity, while the smoothed NEEM levoglucosan strongly peaks (Fig. 3B). This period of decadal-scale
409 increased biomass burning is seen in both the levoglucosan and BC records in the NEEM ice cores, including
410 individual levoglucosan peaks with Z-scores up to 2.8 (Table 1). We infer that the 1500 - 1700 CE maximum in
411 fire activity is due to increased Eurasian boreal forest fires (Figure 3), which are probably underrepresented in
412 the GCD, reflecting the bias in the geographical distribution of GCD sites. Over 50 high latitude North American
413 sites exist yet Siberia only has less than 10 lake cores > 60°N which span a distance of over 7000 km.

414

415 Sapart et al. (2012) argue that changes in the $\delta^{13}\text{C}$ of CH_4 record cannot be explained without biomass burning
416 variability. Methane isotopic variations during the past two millennia (Fig. 3F) correlate with anthropogenic
417 activities, which have contributed to the methane budget before industrial times (Sapart et al., 2012). Methane
418 emissions may be linked to early industrial activity including copper and lead smelting but levoglucosan is not
419 released during coal combustion needed for early industrial activities. Despite the differences in sources and
420 their geographical distribution, the NEEM $\delta^{13}\text{C}$ of CH_4 isotopic record contains similar features to the
421 levoglucosan data (Fig. 3F). High $\delta^{13}\text{C}$ values between 800 - 1200 CE, and to a lesser extent from 100 BCE until
422 200 CE, corresponds with increased levoglucosan and BC concentrations. The pronounced levoglucosan peak
423 centered on ~ 1600 CE only partially overlaps with the pyrogenic methane record, where $\delta^{13}\text{C}$ peaks in the 1400s
424 to 1500s.

425

426 4.3 Source of NEEM fire products

427 4.3.1 Fuel Loads and Circulation Patterns

428 Stable oxygen isotope ($\delta^{18}\text{O}$) data demonstrate that the circulation pattern of air masses reaching the Greenland
429 ice sheet did not significantly change over the last 10,000 years (Vinther et al., 2006). We therefore assume that
430 the atmospheric transport of biomass burning plumes should not have significantly changed during the past two
431 millennia. The isotopic composition of dust in ice cores helps determine the geographic origin of particulate
432 matter reaching Greenland. Holocene mineral dust in the NGRIP (North Greenland Ice core Project) ice core has

433 an Asian origin with the Gobi and Taklimakan deserts as the best source candidates (Bory et al., 2003; Bory et
434 al., 2002; Lupker et al., 2010). These studies argue that North America and North Africa are not potential dust
435 sources, as both regions have higher K/C ratios and higher smectite contents than dust extracted from NGRIP.
436 Although mineral dust and biomass burning products are subject to different transportation styles and
437 atmospheric interactions, these dust studies demonstrate the influence of Asian sources on material transported
438 to the Greenland ice sheet. The Gobi and Taklimakan deserts have very little vegetation and so likely are not
439 biomass burning sources, but these deserts border boreal forest regions that may be important biomass burning
440 sources during major fire events, as discussed throughout this section (Table 2).

441

442 Earth's boreal forests cover 9-12 million km² (Fig. 1), extending across Scandinavia, Russia and North America
443 (NA), representing approximately 10% of Earth land cover and one third of the total global forested area (Zhang
444 et al., 2003; Canadian Forest Canadian Forest Service, 2005). Boreal forest forms a green belt just below the
445 Arctic Circle (55° to 70°N) interrupted only by the Pacific and Atlantic Oceans, and thus forms the major fuel
446 source for fire emissions reaching the Greenland ice sheet. We consider both coniferous and deciduous forests at
447 $\geq 55^\circ$ N as boreal forests (Fig. 1). Russian forests alone represent ~25% of global terrestrial biomass (Zhang et
448 al., 2003). Two thirds of boreal forests are located within the 17 million km² of the Russian Federation (Zhang et
449 al., 2003). Russian boreal forests have a high fire risk due to accumulated organic matter with slow
450 decomposition rates and boreal regions have low precipitation during the summer fire season (Damoah et al.,
451 2004). Canadian boreal forests comprise about one third of the NH circumpolar boreal forest (Canadian Forest
452 Service, 2005).

453

454 Arctic snow samples across the Greenland ice sheet and associated back-trajectories from a single year highlight
455 the importance of Russian boreal forests as a biomass burning source and suggest that 55% of modern BC
456 reaching the Greenland ice sheet originates from Russian biomass burning, while 40% is from North America,
457 and only ~ 5% is from anthropogenic emissions (Hegg et al., 2009). A 44-year record of 10 day isobaric back-
458 trajectories reaching Summit, Greenland (Kahl et al., 1997), indicates that more summer (fire season) trajectories

459 originate over North America (46 % at 500 hPa and 85 % at 700 hPa) than from Eastern Asia (20 % at 500 hPa
460 and 6% at 700 hPa) or from Europe and Western Asia (only 6 % at 500 hPa). The pressure of 500 hPa
461 corresponds to ~ 5 – 6 km asl and is typical of mid-stratospheric circulation, while 700 hPa is closer to the
462 altitude of the Summit camp. A model intercomparison demonstrates that North America and Europe each
463 contribute 40% of the total anthropogenic BC deposited on Greenland (Shindell et al., 2008). These models only
464 investigate anthropogenic sources and explicitly state that biogenic Siberian emissions are not included in their
465 estimates. Back trajectory modeling demonstrates the lack of correlation between BC and the specific coniferous
466 fire marker vanillic acid measured in the Greenland D4 ice core. This lack may result from the majority of BC
467 arriving to Greenland between 1850 to 1950 CE having a North American anthropogenic source, and from 1951
468 CE to the present having an Asian industrial source, separate from any fire activity (McConnell et al., 2007).
469 Therefore, any analysis of Greenland BC from 1850 CE onward should not be considered a purely biomass
470 burning indicator, and the sources for BC and fire emissions may substantially differ.

471

472 4.3.2 *Levoglucosan Sources*

473 Back-trajectory and model analyses suggest that North American and Siberian forests are the dominant sources
474 of biomass burning aerosols. A first-order approximation of aerosol concentrations along a trajectory is function
475 of time where aerosol concentrations decrease exponentially with transport time (Fischer et al., 2007; Hansson,
476 1994). North America is likely the most important contributor due to the proximity to the NEEM location and
477 the shorter routes travelled by aerosols reaching Greenland with respect to Siberian-Eurasian forests, but
478 previous studies also demonstrate that air masses originating in Asia reach Greenland after a few days.
479 Levoglucosan and BC atmospheric lifetimes are on the order of days to less than two weeks (Fraser and
480 Lakshmanan, 2000; Hennigan et al., 2010), suggesting that these back-trajectory and model analyses include all
481 possible levoglucosan and BC source regions. Asia has generally been ignored as a biomass burning aerosol
482 source for Greenland due in part to the days required for air mass travel time compared to the aerosol
483 atmospheric lifetimes. Atmospheric aerosol scavenging and seasonal circulation changes where more air masses
484 originating from Asia pass over Greenland during the winter months (Kahl et al., 1997) limit the quantity of

485 boreal Asian biomass burning products incorporated into the Greenland ice sheet. However, the back trajectory
486 analyses do demonstrate that although Asia is a lesser source, it is a possible aerosol source. Back-trajectories
487 demonstrate that although many air masses originating from Siberia do have to travel eastward to reach
488 Greenland, others have a north-west trajectory that substantially shortens the necessary travel distance (Kahl et
489 al., 1997).

490

491 The correspondence of the major NEEM levoglucosan peaks with periods of extreme droughts in northern
492 central Asia (Table 2) suggests that Asia may be an important fire source during major fire events while North
493 America may be a more important source for background fire activity. Boreal wildfires can generate sufficient
494 sensible heat during the combustion process to initiate deep convection and inject particles into the upper
495 troposphere and lower stratosphere resulting in longer atmospheric lifetimes and more efficient transport of
496 biomass burning aerosols (Damoah et al., 2004; Trentmann et al., 2006; Dentener et al., 2006; Hodzic et al.,
497 2007). Regional droughts result in large amounts of available deadwood as fuel resulting in intense fires capable
498 of generating deep convection (van Mantgem et al., 2009; Westerling et al., 2006; Trentmann et al., 2006;
499 Hodzic et al., 2007). The correspondence between regional droughts and increased fire activity is present in
500 multiple northern and central Asian proxies (Table 2). The Ushkovsky (Kawamura et al., 2012) and Belukha
501 (Eichler et al., 2011) ice cores both contain up to multi-decadal periods of increased fire activity that are similar
502 to peaks in the NEEM ice core suggesting that these sites may receive a contribution from Siberian fire activity
503 (Fig. 3). Our work suggests that Siberia is an important source of burning signatures inferred in Arctic ice fields
504 during extreme fire events.

505

506 *4.4 Climatic and Anthropogenic Influences on Decadal to Centennial Changes in Fire Activity*

507 Fire frequency and intensity depend on regional climatic and environmental influences, where vegetation type,
508 temperature and precipitation are the most important factors. Vegetation distribution impacts levoglucosan
509 emission factors (the amount per kg of burnt fuel) and combustion characteristics (smoldering versus flaming
510 fires) (Simoneit et al., 1999; Engling et al., 2006). Large-scale variations in vegetation types likely do not cause

511 the observed centennial oscillations, but may affect fire signatures over millennial timescales. Instead, elevated
512 surface air temperatures and sustained drought affect fuel flammability and lead to increased global fire activity
513 over seasonal to centennial timescales (Daniau et al., 2012).

514

515 *4.4.1 Temperature*

516 Temperature anomalies during the past 2000 years are not globally synchronous. The regional pattern of the
517 Medieval Warm Period (MWP) results in differing times of maximum warming by region. Global temperature
518 anomalies were highest between 950 - 1250 CE (Mann et al., 2009), whereas northern hemisphere (and
519 especially Russian) temperatures were elevated between 1000 - 1300 CE (Crowley and Lowery, 2000; Hiller et
520 al., 2001) or 1000 - 1100 CE (Moberg et al., 2005). Such temperature anomalies correlate with increased fire
521 activity in paleofire reconstructions inferred from various environmental archives including the Eclipse Icefield
522 in the Yukon, Canada (1240 - 1410 CE) (Yalcin et al., 2006), Eurocore (1200 - 1350 CE) (Savarino and
523 Legrand, 1998) and GISP2 ice cores (1200 - 1600 CE) (Taylor et al., 1996), and in the HLNH > 55° GCD
524 between 1000 - 1400 CE (Marlon et al., 2008).

525

526 The Little Ice Age (LIA) is characterized by relatively cold conditions between 1580 and 1880 CE (Pages 2k,
527 2013) but varies regionally between 1400 - 1700 CE (Mann et al., 2009), 1580 - 1720 CE (Christiansen and
528 Ljungqvist, 2012) or 1350 - 1850 CE (Wanner et al., 2008). Low fire activity is observed in Eurocore (Summit,
529 Greenland) (Savarino and Legrand, 1998) from 1600 - 1850 CE and in the global NH curve (based on GCD
530 syntheses) centered around 1750 CE (Marlon et al., 2008). Comparisons of the levoglucosan profile with a high-
531 latitude northern hemisphere terrestrial temperature anomaly record (Mann et al., 2008) suggests a
532 correspondence between temperature and fire activity observed in the deep NEEM ice core, except during the
533 levoglucosan maximum centered around 1600 CE (Fig. 3E). Fire activity inferred from the deep NEEM ice core
534 is consistent with the MWP and LIA climatic conditions, with high values between the 11th and 13th century and
535 with low decadal-scale levoglucosan concentrations in the 18th century, after removing the individual spikes
536 attributed to mega-events.

537

538 *4.4.2 Precipitation*

539 Ice core, tree-ring proxy records and archival evidences document extensive north-central Asian droughts
540 concurrent with the strongest centennial-scale levoglucosan concentrations during the 16th and 17th centuries
541 including two strong events (1593 - 1603 CE and 1617 - 1622 CE) (Fig. 2, Table 1 and 2). The Siberian
542 Belukha ice core identifies a period of exceptionally high forest-fire activity between 1600 - 1680 CE, following
543 a drought period during 1540 - 1600 CE, which is coincident with elevated NEEM levoglucosan concentrations
544 (Eichler et al., 2011). This period coincides with the Late Ming Weak Monsoon Period (1580 - 1640 CE) (Zhang
545 et al., 2008), which has been invoked as contributing to the decline of the Ming Dynasty. Two central and
546 northern Asian droughts (1586 - 1589 CE and 1638 - 1641 CE) were the most extreme of the past 5 centuries
547 (Shen et al., 2007), yet occurred during relatively cold periods (Li et al., 2009; Cook et al., 2010; Yang et al.,
548 2002; Tan et al., 2003) and covered much of central Asia (Fang et al., 2010). The 1586 - 1589 CE drought
549 resulted in the desiccation of Lake Taihu (the third largest freshwater lake in China) and the even more spatially
550 extensive 1638 - 1641 CE drought event resulted in no outflow of the Yellow River (Shen et al., 2007).
551 Levoglucosan and BC concentrations from the NEEM ice core contain outlying peaks in 1702 - 1706 CE and
552 1787 - 1791 CE, during a period of low centennial-scale fire activity. Paleoclimate reconstructions report
553 extensive drought conditions in China and Mongolia throughout these periods (Table 2). A high-resolution
554 determination of continental dust in the Dye-3 Greenland ice core Sr, Nd and Hf isotopic composition from 1786
555 - 1793 CE determine that the majority of the samples have an Asian origin (Lupker et al., 2010). A network of
556 tree-ring chronologies and historical documents (Grove, 1998; Cook et al., 2010) and the Dasuopu ice core
557 (Thompson et al., 2000) demonstrate that the 1790 - 1796 CE drought was the most intense arid period of the last
558 millennium.

559

560 Major droughts in Asia are associated with summer monsoon failures, and their multi-annual nature suggests that
561 the droughts may have continued to occur through the winter (Table 2). The Siberian High is a seasonal high-
562 pressure system from approximately 70° to 120° E and 45° to 60° N that is the dominant control on northern

563 Asian winter and spring climate (Gong and Ho, 2002; Panagiotopoulos et al., 2005; Sorrel et al., 2007). A
564 stronger winter Siberian High generally results in decreased precipitation and temperatures in the area covered
565 by the high pressure system (Panagiotopoulos et al., 2005; Sorrel et al., 2007; Chen et al., 2010). An enhanced
566 Siberian High during 1330 - 1750 CE is consistent with Aral Sea dust records demonstrating decreased
567 temperatures and a regional drought including decreased Mediterranean precipitation arriving to western Central
568 Asia (Huang et al., 2011; Sorrel et al., 2007) and with increased $nssK^+$ in the GISP2 ice core (Meeker and
569 Mayewski, 2002). Summer Asian monsoon activity correlates with solar variability (Zhang et al., 2008). The
570 northern and central Asian megadroughts coincide with periods of decreased sunspot activity (Weng,
571 2012). Low sunspot activity may increase the strength of the Siberian High (Weng, 2012) and therefore result in
572 decreased precipitation. We suggest that Siberian fire activity is closely related to precipitation changes, where
573 extreme biomass burning peaks are synchronous with precipitation anomalies, independently supporting GISS
574 GCM model results (Pechony and Shindell, 2010).

575

576 North American droughts may have also affected fire activity archived in the NEEM ice cores. Elevated aridity
577 and megadroughts during the MWP (900 - 1300 CE), coincident with levoglucosan peaks, affected large areas of
578 North America and were more prolonged than any 20th century droughts (Cook et al., 2004; Stahle et al., 2000).
579 Dry conditions during the 16th century were also inferred in the Canadian Prairie Provinces (St. George et al.,
580 2009) and in western North America (Stahle et al., 2000). In particular, tree rings from southern Manitoba,
581 Canada, record the lowest growth in 1595 CE (St. George et al., 2009), when a strong fire event is recorded by
582 levoglucosan and ammonium in a 2.20 m NEEM sample dated 1593 - 1603 CE, and by a BC spike in the
583 NEEM-2011-S1 in 1594.5 CE. Levoglucosan spikes in 1704 and 1789 CE are also synchronous with drought
584 periods in the North America, inferred by tree-ring analysis. 1790s was the driest decade in Southwestern
585 Canada (Sauchyn and Skinner, 2001; Sauchyn and Beaudoin, 1998; Wolfe et al., 2001), as in Southern Alberta
586 (Case and Macdonald, 1995). However, St. George et al. (2009) indicate that tree growth was low in 1790s due
587 to dry conditions across the Canadian prairies. The same authors observed a “prolonged absence of wet years

588 around 1700” on the eastern side of the Canadian prairies, where this “notable” dry event lasted between 1688
589 and 1715 CE when tree growth was generally below the mean (St. George et al., 2009).

590

591 4.4.3 *Human impact on boreal fire activity*

592 Climate may be more important than anthropogenic activity in influencing high latitude boreal fires in areas
593 responsible for levoglucosan emissions reaching the Greenland ice sheet even after 1750 CE (Marlon et al.,
594 2008). Linkages between humans and fire regimes are intricate, where increasing population does not necessarily
595 result in enhanced fire activity (Archibald et al., 2009; Prentice, 2010). Marlon et al. (2008) argue that
596 population growth and land-cover conversion rates, along with increases in global temperatures, are the main
597 factors for the sharp increase in global biomass burning from 1750 CE to the late 19th century. However, Marlon
598 et al. (2008) and Prentice (2010) assert that the expansion of agriculture and fire suppression since the early
599 twentieth century resulted in decreased global fire activity, where current biomass burning rates may be lower
600 than over the past 2000 years. These results are supported by South Pole ice core carbon monoxide isotopic data
601 that also record a downturn in global fire activity from the late 1800s to present (Wang et al., 2010). Pyrogenic
602 methane isotopic data (Ferretti et al., 2005; Mischler et al., 2009), which show relatively high values in the first
603 millennium CE, do not support the prominent maximum of an anthropogenic peak at ~ 1900 CE in the HLNH >
604 55° GCD curve (Marlon et al., 2008) and inferred from CO isotopic measurements (Wang et al., 2010), and
605 instead demonstrate that pyrogenic methane sources are still increasing with higher rates than during the last 2
606 millennia. Emissions modeling does not agree with methane isotopes data, and suggests that higher-than-present
607 levels of pre-industrial biomass burning are implausible (van der Werf et al., 2013). Levoglucosan
608 concentrations are relatively high during the past century, but other higher multi-decadal maxima are present in
609 our dataset (Fig. S5). The number of post-1950 CE samples in our data set is limited, and so the levoglucosan
610 analyses in the past decades are not sufficient to clearly assess the 20th century downturn in fire activity.
611 Levoglucosan data do not show the evident anthropogenic peak started from 1750 CE as inferred from the GCD
612 synthesis, as the NEEM levoglucosan profile contains low concentrations until the beginning of the 20th century,
613 followed by a modest concentration increase. No significant increase in fire activity during the past 300 yr is

614 even observed on the Altai region, Southern Siberia (Eichler et al., 2011).

615

616 The differences between the GCD, $\delta^{13}\text{C}$ of CH_4 , and levoglucosan in NEEM may be related to differing
617 initiation times of extensive industrial and agricultural activity in boreal forest source regions. As previously
618 discussed, Russian and Canadian boreal forests are likely the principal sources of levoglucosan reaching the
619 Greenland ice sheet. Population growth and major anthropogenic land clearing in these regions only significantly
620 increased during the past century (Kawamura et al., 2012). The former Soviet Union experienced the highest
621 forest clearing rates and eastward cropland expansion into southern Siberia between 1940 and 1960 CE, while
622 the high Canadian land clearing rates occurred in the prairie provinces between 1900 and 1920 CE (Ramankutty
623 and Foley, 1999). NEEM levoglucosan peaks during the same time interval as these land-clearing estimates.
624 Canadian ice cores also show peak biomass burning from 1920 - 1940 CE (Yalcin et al., 2006) and 1930 - 1980
625 CE (Whitlow et al., 1994).

626

627 The dense GCD sampling in North America and Europe may affect the high latitude Northern Hemisphere
628 charcoal synthesis. The conclusion that land-use and fire management practices decreased global fire activity
629 since the early twenty century (Marlon et al., 2008) may be more appropriate for temperate North America and
630 Europe than for boreal regions. NEEM levoglucosan concentrations may instead reflect the boreal source region
631 land-clearance that was occurring even when anthropogenic land use and fire suppression were dominant in
632 other parts of the Northern Hemisphere.

633

634 **5 Conclusion**

635 Levoglucosan, NH_4^+ and BC analyses in the NEEM ice cores provide a specific record of past biomass burning.
636 Each biomass burning marker has a set of intrinsic strengths and limitations, and so a combination of fire proxies
637 results in a more robust reconstruction. The NEEM records and connections with back trajectories and other
638 paleoclimate studies suggest North American/Canadian fires are the main sources of pyrogenic aerosols
639 transported to the site in particular during the preindustrial period. However, Siberian forests may be an essential
640 aspect of boreal fire reconstructions that have not yet been appropriately evaluated. Temperature may be the
641 controlling factor of boreal fire activity on centennial time scales. On multi-decadal or shorter timescales,
642 however, boreal fires are mainly influenced by precipitation. NEEM levoglucosan, NH_4^+ and BC concentrations
643 suggest the major drought centered on 1640 CE may have been more extensive than inferred from local
644 paleoclimate reconstructions, and that this event dominates boreal fire activity over the past 2000 years.

645

646 Our results demonstrate the greatest amount of decadal-scale fire activity during the mid-1600s. We conclude
647 that the 1500 – 1700 CE maximum in fire activity is due to increased boreal forest fires, caused by extensive dry
648 conditions in the Asian region. Fires are concurrent with known extensive droughts and monsoon failures, and
649 levoglucosan concentrations are greater than during the last 150 years when anthropogenic land-clearing rates
650 were the highest in history. This evidence suggests that climate variability has influenced boreal forest fires more
651 than anthropogenic activity over the past millennia in the boreal regions that supply biomass burning related
652 species to Greenland. However, climate change and anthropogenic activity may increase future boreal fire
653 activity, and have the potential to exceed the fire activity during the mid-1600s. Warmer, drier summers and
654 increased deadwood availability due to past fire suppression, as well as insect outbreaks (Kurz et al., 2008;
655 Wolken et al., 2011), and increased tree mortality from drought (van Mantgem et al., 2009) may amplify current
656 and future fires. Increasing forest mortality in a warming climate (Anderegg et al., 2013) results in greater fuel
657 availability with the potential to intensify future boreal fire activity.

658

659 **6 Acknowledgments**

660 NEEM is directed and organized by the Center of Ice and Climate at the Niels Bohr Institute and US NSF,
661 Office of Polar Programs. The research leading to these results has received funding from the European Union’s
662 Seventh Framework programme (FP7/2007-2013) under grant agreement no. 243908, ”Past4Future. Climate
663 change - Learning from the past climate”, and is Past4Future contribution no. 70. The research leading to these
664 results has received funding from the European Union’s Seventh Framework programme (“Ideas” Specific
665 Programme, ERC Advanced Grant) under grant agreement no 267696 “EARLYhumanIMPACT”. This is
666 EarlyHumanImpact contribution no. 10. US NSF grant 0909541 supported collection and analysis of the NEEM-
667 2011-S1 core. We acknowledge the substantial efforts of the NEEM logistics, drilling, and science trench teams
668 for their substantial efforts during the collection of the NEEM-2011-S1 core, as well as the entire DRI ice core
669 analytical team for their efforts in analyzing the core. Financial support of the Swiss National Science
670 Foundation is acknowledged (Simon Schüpbach). JRM was supported by a United States National Science
671 Foundation Postdoctoral Fellowship (EAR-0948288). We thank PAGES (Past Global Changes) for supporting
672 the paleofire studies development. We also acknowledge Elga (High Wycombe, U.K.) for providing ultrapure
673 water. We thank A. Eichler for the use of their data extracted from (Eichler et al., 2011), and O. Pechony and D.
674 Shindell for the use of their data extracted from (Pechony and Shindell, 2010). We also thank Thomas Blunier
675 and Jerome Chappellaz for the use of their high-resolution NEEM methane data.

676

677 **References**

678

- 679 Anderegg, W. R. L., Kane, J. M., and Anderegg, L. D. L.: Consequences of widespread tree Mortality triggered by drought
680 and temperature stress, *Nat. Clim. Chang.*, 3, 30-36, 2013.
- 681 Andersen, K. K., Ditlevsen, P. D., Rasmussen, S. O., Clausen, H. B., Vinther, B. M., Johnsen, S. J., and Steffensen, J. P.:
682 Retrieving a common accumulation record from Greenland ice cores for the past 1800 years, *J. Geophys. Res.-Atmos.*,
683 111, D15106, doi:10.1029/2005jd006765, 2006.
- 684 Andreev, A. A., Pierau, R., Kalugin, I. A., Daryin, A. V., Smolyaninova, L. G., and Diekmann, B.: Environmental changes
685 in the northern Altai during the last millennium documented in Lake Teletskoye pollen record, *Quat. Res.*, 67, 394-399,
686 10.1016/j.yqres.2006.11.004, 2007.
- 687 Archibald, S., Roy, D. P., van Wilgen, B. W., and Scholes, R. J.: What limits fire? An examination of drivers of burnt area
688 in Southern Africa, *Glob. Change Biol.*, 15, 613-630, 10.1111/j.1365-2486.2008.01754.x, 2009.
- 689 Banta, J. R., McConnell, J. R., Edwards, R., and Engelbrecht, J. P.: Delineation of carbonate dust, aluminous dust, and sea
690 salt deposition in a Greenland glaciochemical array using positive matrix factorization, *Geochem. Geophys. Geosyst.*, 9,
691 Q07013, 10.1029/2007gc001908, 2008.
- 692 Bauer, S. E., Bausch, A., Nazarenko, L., Tsigaridis, K., Xu, B. Q., Edwards, R., Bisiaux, M., and McConnell, J.: Historical
693 and future black carbon deposition on the three ice caps: Ice core measurements and model simulations from 1850 to
694 2100, *J. Geophys. Res.-Atmos.*, 118, 7948-7961, 10.1002/jgrd.50612, 2013.
- 695 Blunier, T., Spahni, R., Barnola, J. M., Chappellaz, J., Loulergue, L., and Schwander, J.: Synchronization of ice core
696 records via atmospheric gases, *Clim. Past.*, 3, 325-330, 2007.
- 697 Bory, A. J. M., Biscaye, P. E., Svensson, A., and Grousset, F. E.: Seasonal variability in the origin of recent atmospheric
698 mineral dust at NorthGRIP, Greenland, *Earth Planet. Sci. Lett.*, 196, 123-134, 10.1016/s0012-821x(01)00609-4, 2002.
- 699 Bory, A. J. M., Biscaye, P. E., Piotrowski, A. M., and Steffensen, J. P.: Regional variability of ice core dust composition
700 and provenance in Greenland, *Geochem. Geophys. Geosyst.*, 4, 1107, 10.1029/2003gc000627, 2003.
- 701 Bowman, D., Balch, J. K., Artaxo, P., Bond, W. J., Carlson, J. M., Cochrane, M. A., D'Antonio, C. M., DeFries, R. S.,
702 Doyle, J. C., Harrison, S. P., Johnston, F. H., Keeley, J. E., Krawchuk, M. A., Kull, C. A., Marston, J. B., Moritz, M. A.,
703 Prentice, I. C., Roos, C. I., Scott, A. C., Swetnam, T. W., van der Werf, G. R., and Pyne, S. J.: Fire in the Earth System,
704 *Science*, 324, 481-484, 10.1126/science.1163886, 2009.
- 705 Brunelle, A., Whitlock, C., Bartlein, P., and Kipfmüller, K.: Holocene fire and vegetation along environmental gradients in
706 the Northern Rocky Mountains, *Quat. Sci. Rev.*, 24, 2281-2300, 10.1016/j.quascirev.2005.11.010, 2005.
- 707 Canadian Forest Service: The State of Canada's Forests 2004-2005: The boreal forest, Ottawa, 2005.
- 708 Case, R. A., and Macdonald, G. M.: A DENDROCLIMATIC RECONSTRUCTION OF ANNUAL PRECIPITATION ON
709 THE WESTERN CANADIAN PRAIRIES SINCE AD 1505 FROM PINUS-FLEXILIS JAMES, *Quat. Res.*, 44, 267-
710 275, 10.1006/qres.1995.1071, 1995.
- 711 Chen, F., Yuan, Y. J., Wen, W. S., Yu, S. L., Fan, Z., Zhang, R. B., Zhang, T. W., and Shang, H. M.: Tree-ring-based
712 reconstruction of precipitation in the Changling Mountains, China, since A.D.1691, *Int. J. Biometeorol.*, 56, 765-774,
713 10.1007/s00484-011-0431-8, 2012.
- 714 Chen, H. F., Song, S. R., Lee, T. Q., Lowemark, L., Chi, Z. Q., Wang, Y., and Hong, E.: A multiproxy lake record from
715 Inner Mongolia displays a late Holocene teleconnection between Central Asian and North Atlantic climates, *Quat. Int.*,
716 227, 170-182, 10.1016/j.quaint.2010.03.005, 2010.
- 717 Christiansen, B., and Ljungqvist, F. C.: The extra-tropical Northern Hemisphere temperature in the last two millennia:
718 reconstructions of low-frequency variability, *Clim. Past.*, 8, 765-786, 10.5194/cp-8-765-2012, 2012.
- 719 Chu, G., Sun, Q., Wang, X., and Sun, J.: Snow anomaly events from historical documents in eastern China during the past
720 two millennia and implication for low-frequency variability of AO/NAO and PDO, *Geophys. Res. Lett.*, 35, L14806,
721 10.1029/2008gl034475, 2008.
- 722 Conard, S. G., Sukhinin, A. I., Stocks, B. J., Cahoon, D. R., Davidenko, E. P., and Ivanova, G. A.: Determining effects of
723 area burned and fire severity on carbon cycling and emissions in Siberia, *Clim. Change*, 55, 197-211,
724 10.1023/a:1020207710195, 2002.
- 725 Conedera, M., Tinner, W., Neff, C., Meurer, M., Dickens, A. F., and Krebs, P.: Reconstructing past fire regimes: methods,
726 applications, and relevance to fire management and conservation, *Quat. Sci. Rev.*, 28, 555-576,
727 10.1016/j.quascirev.2008.11.005, 2009.
- 728 Cook, E. R., Woodhouse, C. A., Eakin, C. M., Meko, D. M., and Stahle, D. W.: Long-term aridity changes in the western
729 United States, *Science*, 306, 1015-1018, 10.1126/science.1102586, 2004.

- 730 Cook, E. R., Anchukaitis, K. J., Buckley, B. M., D'Arrigo, R. D., Jacoby, G. C., and Wright, W. E.: Asian Monsoon Failure
731 and Megadrought During the Last Millennium, *Science*, 328, 486-489, 10.1126/science.1185188, 2010.
- 732 Crowley, T. J., and Lowery, T. S.: How warm was the medieval warm period?, *Ambio*, 29, 51-54, 10.1639/0044-
733 7447(2000)029[0051:hwwtmw]2.0.co;2, 2000.
- 734 Damoah, R., Spichtinger, N., Forster, C., James, P., Mattis, I., Wandinger, U., Beirle, S., Wagner, T., and Stohl, A.: Around
735 the world in 17 days - hemispheric-scale transport of forest fire smoke from Russia in May 2003, *Atmos. Chem. Phys.*,
736 4, 1311-1321, 2004.
- 737 Daniau, A. L., Harrison, S. P., and Bartlein, P. J.: Fire regimes during the Last Glacial, *Quat. Sci. Rev.*, 29, 2918-2930,
738 10.1016/j.quascirev.2009.11.008, 2010.
- 739 Daniau, A. L., Bartlein, P. J., Harrison, S. P., Prentice, I. C., Brewer, S., Friedlingstein, P., Harrison-Prentice, T. I., Inoue, J.,
740 Izumi, K., Marlon, J. R., Mooney, S., Power, M. J., Stevenson, J., Tinner, W., Andrić, M., Atanassova, J., Behling, H.,
741 Black, M., Blarquez, O., Brown, K. J., Carcaillet, C., Colhoun, E. A., Colombaroli, D., Davis, B. A. S., D'Costa, D.,
742 Dodson, J., Dupont, L., Eshetu, Z., Gavin, D. G., Genries, A., Haberle, S., Hallett, D. J., Hope, G., Horn, S. P., Kassa, T.
743 G., Katamura, F., Kennedy, L. M., Kershaw, P., Krivonogov, S., Long, C., Magri, D., Marinova, E., McKenzie, G. M.,
744 Moreno, P. I., Moss, P., Neumann, F. H., Norström, E., Páitre, C., Rius, D., Roberts, N., Robinson, G. S., Sasaki, N.,
745 Scott, L., Takahara, H., Terwilliger, V., Thevenon, F., Turner, R., Valsecchi, V. G., Vannièrè, B., Walsh, M., Williams,
746 N., and Zhang, Y.: Predictability of biomass burning in response to climate changes, *Glob. Biogeochem. Cycle*, 26,
747 GB4007, 10.1029/2011GB004249, 2012.
- 748 Davi, N., Jacoby, G., Fang, K., Li, J., D'Arrigo, R., Baatarbileg, N., and Robinson, D.: Reconstructing drought variability
749 for Mongolia based on a large-scale tree ring network: 1520-1993, *J. Geophys. Res.-Atmos.*, 115, D22103,
750 10.1029/2010jd013907, 2010.
- 751 de Groot, W. J., Cantin, A. S., Flannigan, M. D., Soja, A. J., Gowman, L. M., and Newbery, A.: A comparison of Canadian
752 and Russian boreal forest fire regimes, *For. Ecol. Manage.*, 294, 23-34, 10.1016/j.foreco.2012.07.033, 2013.
- 753 Dentener, F., Kinne, S., Bond, T., Boucher, O., Cofala, J., Generoso, S., Ginoux, P., Gong, S., Hoelzemann, J. J., Ito, A.,
754 Marelli, L., Penner, J. E., Putaud, J. P., Textor, C., Schulz, M., van der Werf, G. R., and Wilson, J.: Emissions of
755 primary aerosol and precursor gases in the years 2000 and 1750 prescribed data-sets for AeroCom, *Atmos. Chem. Phys.*,
756 6, 4321-4344, 2006.
- 757 Diamond, J. M.: *Collapse: How Societies Choose to Fail Or Succeed*, Viking, New York, 2005.
- 758 Dibb, J. E., Talbot, R. W., Whitlow, S. I., Shipham, M. C., Winterle, J., McConnell, J., and Bales, R.: Biomass burning
759 signatures in the atmosphere and snow at Summit, Greenland: An event on 5 August 1994, *Atmos. Environ.*, 30, 553-
760 561, 1996.
- 761 Dronin, N. M., and Bellinger, E. G.: *Climate Dependence and Food Problems in Russia, 1900-1990: The Interaction of*
762 *Climate and Agricultural Policy and Their Effect on Food Problems*, Central European University Press, Budepest,
763 Hungary, 2005.
- 764 Eichler, A., Tinner, W., Brusch, S., Olivier, S., Papina, T., and Schwikowski, M.: An ice-core based history of Siberian
765 forest fires since AD 1250, *Quat. Sci. Rev.*, 30, 1027-1034, 10.1016/j.quascirev.2011.02.007, 2011.
- 766 Engling, G., Carrico, C. M., Kreidenweis, S. M., Collett, J. L., Day, D. E., Malm, W. C., Lincoln, E., Hao, W. M., Iinuma,
767 Y., and Herrmann, H.: Determination of levoglucosan in biomass combustion aerosol by high-performance anion-
768 exchange chromatography with pulsed amperometric detection, *Atmos. Environ.*, 40, S299-S311,
769 10.1016/j.atmosenv.2005.12.069, 2006.
- 770 Fang, K. Y., Davi, N., Gou, X. H., Chen, F. H., Cook, E., Li, J. B., and D'Arrigo, R.: Spatial drought reconstructions for
771 central High Asia based on tree rings, *Clim. Dyn.*, 35, 941-951, 10.1007/s00382-009-0739-9, 2010.
- 772 Fang, K. Y., Gou, X., Chen, F., Frank, D., Liu, C., Li, J., and Kazmer, M.: Precipitation variability during the past 400 years
773 in the Xiaolong Mountain (central China) inferred from tree rings, *Clim. Dyn.*, 39, 1697-1707, 10.1007/s00382-012-
774 1371-7, 2012.
- 775 FAO: *Fire management: Global assessment 2006*, Food and Agriculture Organization of the United Nations, Rome, 2007.
- 776 Feng, S., Hu, Q., and Oglesby, R. J.: Influence of Atlantic sea surface temperatures on persistent drought in North America,
777 *Clim. Dyn.*, 37, 569-586, 10.1007/s00382-010-0835-x, 2011.
- 778 Ferretti, D. F., Miller, J. B., White, J. W. C., Etheridge, D. M., Lassey, K. R., Lowe, D. C., Meure, C. M. M., Dreier, M. F.,
779 Trudinger, C. M., van Ommen, T. D., and Langenfelds, R. L.: Unexpected changes to the global methane budget over
780 the past 2000 years, *Science*, 309, 1714-1717, 10.1126/science.1115193, 2005.
- 781 Fischer, H., Siggaard-Andersen, M. L., Ruth, U., Rothlisberger, R., and Wolff, E.: Glacial/interglacial changes in mineral
782 dust and sea-salt records in polar ice cores: Sources, transport, and deposition, *Rev. Geophys.*, 45, RG1002,
783 10.1029/2005rg000192, 2007.
- 784 Fischer, H., Behrens, M., Bock, M., Richter, U., Schmitt, J., Loulergue, L., Chappellaz, J., Spahni, R., Blunier, T.,
785 Leuenberger, M., and Stocker, T. F.: Changing boreal methane sources and constant biomass burning during the last
786 termination, *Nature*, 452, 864-867, 10.1038/nature06825, 2008.

787 Flanner, M. G., Zender, C. S., Randerson, J. T., and Rasch, P. J.: Present-day climate forcing and response from black
788 carbon in snow, *J. Geophys. Res.-Atmos.*, 112, 10.1029/2006jd008003, 2007.

789 Fraser, M. P., and Lakshmanan, K.: Using levoglucosan as a molecular marker for the long-range transport of biomass
790 combustion aerosols, *Environ. Sci. Technol.*, 34, 4560-4564, 10.1021/es991229l, 2000.

791 Fuhrer, K., Neftel, A., Anklin, M., and Maggi, V.: continuous measurements of hydrogen-peroxide, formaldehyde, calcium
792 and ammonium concentrations along the new grip ice core from summit, central greenland, *Atmospheric Environment*
793 *Part a-General Topics*, 27, 1873-1880, 10.1016/0960-1686(93)90292-7, 1993.

794 Fuhrer, K., Neftel, A., Anklin, M., Staffelbach, T., and Legrand, M.: High-resolution ammonium ice core record covering a
795 complete glacial-interglacial cycle, *J. Geophys. Res.-Atmos.*, 101, 4147-4164, 1996.

796 Fuhrer, K., and Legrand, M.: Continental biogenic species in the Greenland Ice Core Project ice core: Tracing back the
797 biomass history of the North American continent, *J. Geophys. Res.-Oceans*, 102, 26735-26745, 1997.

798 Gambaro, A., Zangrando, R., Gabrielli, P., Barbante, C., and Cescon, P.: Direct determination of levoglucosan at the
799 picogram per milliliter level in Antarctic ice by high-performance liquid chromatography/electrospray ionization triple
800 quadrupole mass spectrometry, *Anal. Chem.*, 80, 1649-1655, 10.1021/ac701655x, 2008.

801 Gao, S., Hegg, D. A., Hobbs, P. V., Kirchstetter, T. W., Magi, B. I., and Sadilek, M.: Water-soluble organic components in
802 aerosols associated with savanna fires in southern Africa: Identification, evolution, and distribution, *J. Geophys. Res.-*
803 *Atmos.*, 108, 8491, 10.1029/2002jd002324, 2003.

804 Generoso, S., Bey, I., Attie, J. L., and Breon, F. M.: A satellite- and model-based assessment of the 2003 Russian fires:
805 Impact on the Arctic region, *J. Geophys. Res.-Atmos.*, 112, 10.1029/2006jd008344, 2007.

806 Goldberg, E. D.: *Black carbon in the environment: properties and distribution*, J. Wiley, New York, 1985.

807 Golubev, G., and Dronin, N. M.: *Geography of Droughts and Food Problems in Russia (1900-2000)*. Report of the
808 International Project on Global Environmental Change and Its Threat to Food and Water Security in Russia. Department
809 of Geography, Moscow State University, Moscow, Russia, 2004.

810 Gong, D. Y., and Ho, C. H.: The Siberian High and climate change over middle to high latitude Asia, *Theor. Appl.*
811 *Climatol.*, 72, 1-9, 10.1007/s007040200008, 2002.

812 Grove, R. H.: Global impact of the 1789-93 El Nino, *Nature*, 393, 318-319, 10.1038/30636, 1998.

813 Hallett, D. J., Lepofsky, D. S., Mathewes, R. W., and Lertzman, K. P.: 11 000 years of fire history and climate in the
814 mountain hemlock rain forests of southwestern British Columbia based on sedimentary charcoal, *Can. J. For. Res.-Rev.*
815 *Can. Rech. For.*, 33, 292-312, 10.1139/x02-177, 2003.

816 Hansen, J., and Nazarenko, L.: Soot climate forcing via snow and ice albedos, *Proc. Natl. Acad. Sci. U. S. A.*, 101, 423-428,
817 10.1073/pnas.2237157100, 2004.

818 Hansson, M. E.: The renland ice core - a Northern-Hemisphere record of aerosol composition over 120,000 years, *Tellus*
819 *Ser. B-Chem. Phys. Meteorol.*, 46, 390-418, 10.1034/j.1600-0889.1994.t01-4-00005.x, 1994.

820 Hegg, D. A., Warren, S. G., Grenfell, T. C., Doherty, S. J., Larson, T. V., and Clarke, A. D.: Source Attribution of Black
821 Carbon in Arctic Snow, *Environ. Sci. Technol.*, 43, 4016-4021, 10.1021/es803623f, 2009.

822 Hennigan, C. J., Sullivan, A. P., Collett, J. L., and Robinson, A. L.: Levoglucosan stability in biomass burning particles
823 exposed to hydroxyl radicals, *Geophys. Res. Lett.*, 37, L09806, 10.1029/2010gl043088, 2010.

824 Herron, M. M., and Langway Jr, C. C.: Firm densification: an empirical model, *J. Glaciol.*, 25, 373-385, 1980.

825 Hiller, A., Boettger, T., and Kremenetski, C.: Mediaeval climatic warming recorded by radiocarbon dated alpine tree-line
826 shift on the Kola Peninsula, Russia, Holocene, 11, 491-497, 10.1191/095968301678302931, 2001.

827 Hodzic, A., Madronich, S., Bohn, B., Massie, S., Menut, L., and Wiedinmyer, C.: Wildfire particulate matter in Europe
828 during summer 2003: meso-scale modeling of smoke emissions, transport and radiative effects, *Atmos. Chem. Phys.*, 7,
829 4043-4064, 2007.

830 Hoffmann, D., Tilgner, A., Iinuma, Y., and Herrmann, H.: Atmospheric Stability of Levoglucosan: A Detailed Laboratory
831 and Modeling Study, *Environ. Sci. Technol.*, 44, 694-699, 10.1021/es902476f, 2010.

832 Holmes, B. J., and Petrucci, G. A.: Water-soluble oligomer formation from acid-catalyzed reactions of levoglucosan in
833 proxies of atmospheric aqueous aerosols, *Environ. Sci. Technol.*, 40, 4983-4989, 10.1021/es060646c, 2006.

834 Holmes, B. J., and Petrucci, G. A.: Oligomerization of levoglucosan by Fenton chemistry in proxies of biomass burning
835 aerosols, *J. Atmos. Chem.*, 58, 151-166, 10.1007/s10874-007-9084-8, 2007.

836 Huang, X. T., Oberhansli, H., von Suchodoletz, H., and Sorrel, P.: Dust deposition in the Aral Sea: implications for changes
837 in atmospheric circulation in central Asia during the past 2000 years, *Quat. Sci. Rev.*, 30, 3661-3674,
838 10.1016/j.quascirev.2011.09.011, 2011.

839 Iinuma, Y., Brüggemann, E., Gnauk, T., Müller, K., Andreae, M. O., Helas, G., Parmar, R., and Herrmann, H.: Source
840 characterization of biomass burning particles: The combustion of selected European conifers, African hardwood,
841 savanna grass, and German and Indonesian peat, *J. Geophys. Res.-Atmos.*, 112, D08209, 10.1029/2006jd007120, 2007.

842 IPCC: Climate Change 2013: The Scientific Basis. Contribution of Working Group I to the Fifth Assessment Report of the
843 Intergovernmental Panel on Climate Change [Stocker, T.F., D. Qin, G.-K. Plattner, M. Tignor, S.K. Allen, J.
844 Boschung, A. Nauels, Y. Xia, V. Bex and P.M. Midgley (eds.)], 2013.

845 Jacobson, M. Z.: The short-term cooling but long-term global warming due to biomass burning, *J. Clim.*, 17, 2909-2926,
846 10.1175/1520-0442(2004)017<2909:tscblg>2.0.co;2, 2004.

847 Jaffrezo, J. L., Davidson, C. I., Kuhns, H. D., Bergin, M. H., Hillamo, R., Maenhaut, W., Kahl, J. W., and Harris, J. M.:
848 Biomass burning signatures in the atmosphere of central Greenland, *J. Geophys. Res.-Atmos.*, 103, 31067-31078, 1998.

849 Kahl, J. D. W., Martinez, D. A., Kuhns, H., Davidson, C. I., Jaffrezo, J. L., and Harris, J. M.: Air mass trajectories to
850 Summit, Greenland: A 44-year climatology and some episodic events, *J. Geophys. Res.-Oceans*, 102, 26861-26875,
851 10.1029/97jc00296, 1997.

852 Kaplan, J. O., Krumhardt, K. M., Ellis, E. C., Ruddiman, W. F., Lemmen, C., and Goldewijk, K. K.: Holocene carbon
853 emissions as a result of anthropogenic land cover change, *Holocene*, 21, 775-791, 10.1177/0959683610386983, 2011.

854 Kaufmann, P. R., Federer, U., Hutterli, M. A., Bigler, M., Schupbach, S., Ruth, U., Schmitt, J., and Stocker, T. F.: An
855 Improved Continuous Flow Analysis System for High-Resolution Field Measurements on Ice Cores, *Environ. Sci.*
856 *Technol.*, 42, 8044-8050, 10.1021/es8007722, 2008.

857 Kawamura, K., Yokoyama, K., Fujii, Y., and Watanabe, O.: A Greenland ice core record of low molecular weight
858 dicarboxylic acids, ketocarboxylic acids, and alpha-dicarbonyls: A trend from Little Ice Age to the present (1540 to
859 1989 AD), *J. Geophys. Res.-Atmos.*, 106, 1331-1345, 2001.

860 Kawamura, K., Izawa, Y., Mochida, M., and Shiraiwa, T.: Ice core records of biomass burning tracers (levoglucosan and
861 dehydroabietic, vanillic and p-hydroxybenzoic acids) and total organic carbon for past 300 years in the Kamchatka
862 Peninsula, Northeast Asia, *Geochim. Cosmochim. Acta*, 99, 317 - 329, 10.1016/j.gca.2012.08.006, 2012.

863 Kehrwald, N., Zangrando, R., Gabrielli, P., Jaffrezo, J. L., Boutron, C., Barbante, C., and Gambaro, A.: Levoglucosan as a
864 specific marker of fire events in Greenland snow, *Tellus Ser. B-Chem. Phys. Meteorol.*, 64, 18196,
865 10.3402/tellusb.v64i0.18196, 2012.

866 Kuo, L. J., Herbert, B. E., and Louchouart, P.: Can levoglucosan be used to characterize and quantify char/charcoal black
867 carbon in environmental media?, *Org. Geochem.*, 39, 1466-1478, 10.1016/j.orggeochem.2008.04.026, 2008.

868 Kurz, W. A., Stinson, G., Rampley, G. J., Dymond, C. C., and Neilson, E. T.: Risk of natural disturbances makes future
869 contribution of Canada's forests to the global carbon cycle highly uncertain, *Proc. Natl. Acad. Sci. U. S. A.*, 105, 1551-
870 1555, 10.1073/pnas.0708133105, 2008.

871 Lavoue, D., Lioussé, C., Cachier, H., Stocks, B. J., and Goldammer, J. G.: Modeling of carbonaceous particles emitted by
872 boreal and temperate wildfires at northern latitudes, *J. Geophys. Res.-Atmos.*, 105, 26871-26890,
873 10.1029/2000jd900180, 2000.

874 Legrand, M., Deangelis, M., Staffelbach, T., Neftel, A., and Stauffer, B.: Large perturbation of ammonium and organic-
875 acids content in the Summit-Greenland ice core - Fingerprint from forest-fires, *Geophys. Res. Lett.*, 19, 473-475, 1992.

876 Legrand, M., Angelis, M., Cachier, H., and Gaudichet, A.: Boreal Biomass Burning Over the Last 80 Years Recorded in a
877 Summit-Greenland Ice Core, in: *Ice Core Studies of Global Biogeochemical Cycles*, edited by: Delmas, R., NATO ASI
878 Series, Springer Berlin Heidelberg, 347-360, 1995.

879 Legrand, M., and DeAngelis, M.: Light carboxylic acids in Greenland ice: A record of past forest fires and vegetation
880 emissions from the boreal zone, *J. Geophys. Res.-Atmos.*, 101, 4129-4145, 1996.

881 Li, J. B., Cook, E. R., Chen, F. H., Davi, N., D'Arrigo, R., Gou, X. H., Wright, W. E., Fang, K. Y., Jin, L. Y., Shi, J. F., and
882 Yang, T.: Summer monsoon moisture variability over China and Mongolia during the past four centuries, *Geophys. Res.*
883 *Lett.*, 36, L22705, 10.1029/2009gl041162, 2009.

884 Liu, Y., Shi, J. F., Shishov, V., Vaganov, E., Yang, Y. K., Cai, Q. F., Sun, J. Y., Wang, L., and Djanseitov, I.:
885 Reconstruction of May-July precipitation in the north Helan Mountain, Inner Mongolia since AD 1726 from tree-ring
886 late-wood widths, *Chin. Sci. Bull.*, 49, 405-409, 10.1007/BF02900325, 2004.

887 Liu, Y., Tian, H., Song, H. M., and Liang, J. M.: Tree ring precipitation reconstruction in the Chifeng-Weichang region,
888 China, and East Asian summer monsoon variation since AD 1777, *J. Geophys. Res.-Atmos.*, 115, D06103,
889 10.1029/2009jd012330, 2010.

890 Lupker, M., Aciego, S. M., Bourdon, B., Schwander, J., and Stocker, T. F.: Isotopic tracing (Sr, Nd, U and Hf) of
891 continental and marine aerosols in an 18th century section of the Dye-3 ice core (Greenland), *Earth Planet. Sci. Lett.*,
892 295, 277-286, 10.1016/j.epsl.2010.04.010, 2010.

893 Mann, M. E., Zhang, Z. H., Hughes, M. K., Bradley, R. S., Miller, S. K., Rutherford, S., and Ni, F. B.: Proxy-based
894 reconstructions of hemispheric and global surface temperature variations over the past two millennia, *Proc. Natl. Acad.*
895 *Sci. U. S. A.*, 105, 13252-13257, 10.1073/pnas.0805721105, 2008.

896 Mann, M. E., Zhang, Z. H., Rutherford, S., Bradley, R. S., Hughes, M. K., Shindell, D., Ammann, C., Faluvegi, G., and Ni,
897 F. B.: Global Signatures and Dynamical Origins of the Little Ice Age and Medieval Climate Anomaly, *Science*, 326,
898 1256-1260, 10.1126/science.1177303, 2009.

899 Marlon, J. R., Bartlein, P. J., Carcaillet, C., Gavin, D. G., Harrison, S. P., Higuera, P. E., Joos, F., Power, M. J., and
900 Prentice, I. C.: Climate and human influences on global biomass burning over the past two millennia, *Nat. Geosci.*, 1,
901 697-702, 10.1038/ngeo313, 2008.

902 Marlon, J. R., Bartlein, P. J., Gavin, D. G., Long, C. J., Anderson, R. S., Briles, C. E., Brown, K. J., Colombaroli, D.,
903 Hallett, D. J., Power, M. J., Scharf, E. A., and Walsh, M. K.: Long-term perspective on wildfires in the western USA,
904 *Proc. Natl. Acad. Sci. U. S. A.*, 109, E535-E543, 10.1073/pnas.1112839109, 2012.

905 Marlon, J. R., Bartlein, P. J., Daniau, A. L., Harrison, S. P., Maezumi, S. Y., Power, M. J., Tinner, W., and Vanniére, B.:
906 Global biomass burning: a synthesis and review of Holocene paleofire records and their controls, *Quat. Sci. Rev.*, 65, 5-
907 25, 10.1016/j.quascirev.2012.11.029, 2013.

908 Masiello, C. A.: New directions in black carbon organic geochemistry, *Mar. Chem.*, 92, 201-213,
909 10.1016/j.marchem.2004.06.043, 2004.

910 McConnell, J. R.: Continuous ice-core chemical analyses using inductively Coupled Plasma Mass Spectrometry,
911 *Environmental Science & Technology*, 36, 7-11, 10.1021/es011088z, 2002.

912 McConnell, J. R., Edwards, R., Kok, G. L., Flanner, M. G., Zender, C. S., Saltzman, E. S., Banta, J. R., Pasteris, D. R.,
913 Carter, M. M., and Kahl, J. D. W.: 20th-century industrial black carbon emissions altered arctic climate forcing, *Science*,
914 317, 1381-1384, 10.1126/science.1144856, 2007.

915 McConnell, J. R., and Edwards, R.: Coal burning leaves toxic heavy metal legacy in the Arctic, *Proc. Natl. Acad. Sci. U. S.*
916 *A.*, 105, 12140-12144, 10.1073/pnas.0803564105, 2008.

917 McConnell, J. R.: New Directions: Historical black carbon and other ice core aerosol records in the Arctic for GCM
918 evaluation, *Atmos. Environ.*, 44, 2665-2666, 10.1016/j.atmosenv.2010.04.004, 2010.

919 McWethy, D. B., Whitlock, C., Wilmshurst, J. M., McGlone, M. S., and Li, X.: Rapid deforestation of South Islands, New
920 Zealand, by early Polynesian fires, Holocene, 19, 883-897, 10.1177/0959683609336563, 2009.

921 Meeker, L. D., and Mayewski, P. A.: A 1400-year high-resolution record of atmospheric circulation over the North Atlantic
922 and Asia, Holocene, 12, 257-266, 10.1191/0959683602hl542ft, 2002.

923 Melott, A. L., Thomas, B. C., Dreschhoff, G., and Johnson, C. K.: Cometary airbursts and atmospheric chemistry: Tunguska
924 and a candidate Younger Dryas event, *Geology*, 38, 355-358, 10.1130/g30508.1, 2010.

925 Mischler, J. A., Sowers, T. A., Alley, R. B., Battle, M., McConnell, J. R., Mitchell, L., Popp, T., Sofen, E., and Spencer, M.
926 K.: Carbon and hydrogen isotopic composition of methane over the last 1000 years, *Glob. Biogeochem. Cycle*, 23,
927 GB4024, 10.1029/2009gb003460, 2009.

928 Moberg, A., Sonechkin, D. M., Holmgren, K., Datsenko, N. M., and Karlen, W.: Highly variable Northern Hemisphere
929 temperatures reconstructed from low- and high-resolution proxy data, *Nature*, 433, 613-617, 10.1038/nature03265,
930 2005.

931 Mochida, M., Kawamura, K., Fu, P. Q., and Takemura, T.: Seasonal variation of levoglucosan in aerosols over the western
932 North Pacific and its assessment as a biomass-burning tracer, *Atmos. Environ.*, 44, 3511-3518,
933 10.1016/j.atmosenv.2010.06.017, 2010.

934 O'Brien, S. R., Mayewski, P. A., Meeker, L. D., Meese, D. A., Twickler, M. S., and Whitlow, S. I.: Complexity of holocene
935 climate as reconstructed from a greenland ice core, *Science*, 270, 1962-1964, 10.1126/science.270.5244.1962, 1995.

936 Oros, D. R., and Simoneit, B. R. T.: Identification and emission factors of molecular tracers in organic aerosols from
937 biomass burning Part 2. Deciduous trees, *Appl. Geochem.*, 16, 1545-1565, 10.1016/s0883-2927(01)00022-1, 2001a.

938 Oros, D. R., and Simoneit, B. R. T.: Identification and emission factors of molecular tracers in organic aerosols from
939 biomass burning Part 1. Temperate climate conifers, *Appl. Geochem.*, 16, 1513-1544, 10.1016/s0883-2927(01)00021-x,
940 2001b.

941 Pages 2k: Continental-scale temperature variability during the past two millennia, *Nat. Geosci.*, 6, 339-346,
942 10.1038/ngeo1797, <http://www.nature.com/ngeo/journal/v6/n5/abs/ngeo1797.html> -
943 [supplementary information](#), 2013.

944 Panagiotopoulos, F., Shahgedanova, M., Hannachi, A., and Stephenson, D. B.: Observed trends and teleconnections of the
945 Siberian high: A recently declining center of action, *J. Clim.*, 18, 1411-1422, 10.1175/jcli3352.1, 2005.

946 Paris, J. D., Stohl, A., Nedelec, P., Arshinov, M. Y., Panchenko, M. V., Shmargunov, V. P., Law, K. S., Belan, B. D., and
947 Ciais, P.: Wildfire smoke in the Siberian Arctic in summer: source characterization and plume evolution from airborne
948 measurements, *Atmos. Chem. Phys.*, 9, 9315-9327, 2009.

949 Pechony, O., and Shindell, D. T.: Driving forces of global wildfires over the past millennium and the forthcoming century,
950 *Proc. Natl. Acad. Sci. U. S. A.*, 107, 19167-19170, 10.1073/pnas.1003669107, 2010.

951 Pederson, N., Jacoby, G. C., D'Arrigo, R. D., Cook, E. R., Buckley, B. M., Dugarjav, C., and Mijiddorj, R.:
952 Hydrometeorological reconstructions for northeastern Mongolia derived from tree rings: 1651-1995, *J. Clim.*, 14, 872-
953 881, 10.1175/1520-0442(2001)014<0872:hfrnmd>2.0.co;2, 2001.

954 Power, M. J., Marlon, J., Ortiz, N., Bartlein, P. J., Harrison, S. P., Mayle, F. E., Ballouche, A., Bradshaw, R. H. W.,
955 Carcaillet, C., Cordova, C., Mooney, S., Moreno, P. I., Prentice, I. C., Thonicke, K., Tinner, W., Whitlock, C., Zhang,
956 Y., Zhao, Y., Ali, A. A., Anderson, R. S., Beer, R., Behling, H., Briles, C., Brown, K. J., Brunelle, A., Bush, M., Camill,
957 P., Chu, G. Q., Clark, J., Colombaroli, D., Connor, S., Daniau, A. L., Daniels, M., Dodson, J., Doughty, E., Edwards, M.
958 E., Finsinger, W., Foster, D., Frechette, J., Gaillard, M. J., Gavin, D. G., Gobet, E., Haberle, S., Hallett, D. J., Higuera,
959 P., Hope, G., Horn, S., Inoue, J., Kaltenrieder, P., Kennedy, L., Kong, Z. C., Larsen, C., Long, C. J., Lynch, J., Lynch, E.
960 A., McGlone, M., Meeks, S., Mensing, S., Meyer, G., Minckley, T., Mohr, J., Nelson, D. M., New, J., Newnham, R.,
961 Noti, R., Oswald, W., Pierce, J., Richard, P. J. H., Rowe, C., Goni, M. F. S., Shuman, B. N., Takahara, H., Toney, J.,
962 Turney, C., Urrego-Sanchez, D. H., Umbanhowar, C., Vandergoes, M., Vanniere, B., Vescovi, E., Walsh, M., Wang, X.,
963 Williams, N., Wilmshurst, J., and Zhang, J. H.: Changes in fire regimes since the Last Glacial Maximum: an assessment
964 based on a global synthesis and analysis of charcoal data, *Clim. Dyn.*, 30, 887-907, 10.1007/s00382-007-0334-x, 2008.

965 Power, M. J., Marlon, J. R., Bartlein, P. J., and Harrison, S. P.: Fire history and the Global Charcoal Database: A new tool
966 for hypothesis testing and data exploration, *Paleogeogr. Paleoclimatol. Paleocol.*, 291, 52-59,
967 10.1016/j.palaeo.2009.09.014, 2010.

968 Prentice, I. C.: The Burning Issue, *Science*, 330, 1636-1637, 10.1126/science.1199809, 2010.

969 Preston, C. M., and Schmidt, M. W. I.: Black (pyrogenic) carbon: a synthesis of current knowledge and uncertainties with
970 special consideration of boreal regions, *Biogeosciences*, 3, 397-420, 2006.

971 Pyne, S. J.: The fires this time, and next, *Science*, 294, 1005-1006, 10.1126/science.1064989, 2001.

972 Quinn, P. K., Bates, T. S., Baum, E., Doubleday, N., Fiore, A. M., Flanner, M., Fridlind, A., Garrett, T. J., Koch, D.,
973 Menon, S., Shindell, D., Stohl, A., and Warren, S. G.: Short-lived pollutants in the Arctic: their climate impact and
974 possible mitigation strategies, *Atmos. Chem. Phys.*, 8, 1723-1735, 10.5194/acp-8-1723-2008, 2008.

975 Ramanathan, V., and Carmichael, G.: Global and regional climate changes due to black carbon, *Nat. Geosci.*, 1, 221-227,
976 10.1038/ngeo156, 2008.

977 Ramankutty, N., and Foley, J. A.: Estimating historical changes in global land cover: Croplands from 1700 to 1992, *Glob.*
978 *Biogeochem. Cycle*, 13, 997-1027, 10.1029/1999gb900046, 1999.

979 Randerson, J. T., Liu, H., Flanner, M. G., Chambers, S. D., Jin, Y., Hess, P. G., Pfister, G., Mack, M. C., Treseder, K. K.,
980 Welp, L. R., Chapin, F. S., Harden, J. W., Goulden, M. L., Lyons, E., Neff, J. C., Schuur, E. A. G., and Zender, C. S.:
981 The impact of boreal forest fire on climate warming, *Science*, 314, 1130-1132, 10.1126/science.1132075, 2006.

982 Rasmussen, S. O., Abbott, P., Blunier, T., Bourne, A., Brook, E., Buchardt, S. L., Buizert, C., Chappellaz, J., Clausen, H.
983 B., Cook, E., Dahl-Jensen, D., Davies, S., Guillevic, M., Kipfstuhl, S., Laepple, T., Seierstad, I. K., Severinghaus, J. P.,
984 Steffensen, J. P., Stowasser, C., Svensson, A., Vallelonga, P., Vinther, B. M., Wilhelms, F., and Winstrup, M.: A first
985 chronology for the NEEM ice core, *Clim. Past Discuss.*, 9, 2967-3013, 10.5194/cpd-9-2967-2013, 2013.

986 Ruddiman, W. F.: The anthropogenic greenhouse era began thousands of years ago, *Clim. Change*, 61, 261-293,
987 10.1023/B:CLIM.0000004577.17928.fa, 2003.

988 Running, S. W.: Is global warming causing more, larger wildfires?, *Science*, 313, 927-928, 10.1126/science.1130370, 2006.

989 Ruth, U., Wagenbach, D., Steffensen, J. P., and Bigler, M.: Continuous record of microparticle concentration and size
990 distribution in the central Greenland NGRIP ice core during the last glacial period, *J. Geophys. Res.-Atmos.*, 108,
991 10.1029/2002jd002376, 2003.

992 Sapart, C. J., Monteil, G., Prokopiou, M., van de Wal, R. S. W., Kaplan, J. O., Sperlich, P., Krumhardt, K. M., van der
993 Veen, C., Houweling, S., Krol, M. C., Blunier, T., Sowers, T., Martinerie, P., Witrant, E., Dahl-Jensen, D., and
994 Rockmann, T.: Natural and anthropogenic variations in methane sources during the past two millennia, *Nature*, 490, 85-
995 88, <http://www.nature.com/nature/journal/v490/n7418/abs/nature11461.html>
996 [supplementary information](#), 2012.

997 Sauchyn, D. J., and Beaudoin, A. B.: Recent environmental change in the southwestern Canadian Plains, *Can. Geogr.-*
998 *Geogr. Can.*, 42, 337-353, 10.1111/j.1541-0064.1998.tb01350.x, 1998.

999 Sauchyn, D. J., and Skinner, W. R.: A Proxy Record of Drought Severity for the Southwestern Canadian Plains, *Canadian*
1000 *Water Resources Journal*, 26, 253-272, 10.4296/cwrj2602253, 2001.

1001 Savarino, J., and Legrand, M.: High northern latitude forest fires and vegetation emissions over the last millennium inferred
1002 from the chemistry of a central Greenland ice core, *J. Geophys. Res.-Atmos.*, 103, 8267-8279, 1998.

1003 Shen, C., Wang, W.-C., Hao, Z., and Gong, W.: Exceptional drought events over eastern China during the last five
1004 centuries, *Clim. Change*, 85, 453-471, 10.1007/s10584-007-9283-y, 2007.

1005 Shindell, D. T., Chin, M., Dentener, F., Doherty, R. M., Faluvegi, G., Fiore, A. M., Hess, P., Koch, D. M., MacKenzie, I.
1006 A., Sanderson, M. G., Schultz, M. G., Schulz, M., Stevenson, D. S., Teich, H., Textor, C., Wild, O., Bergmann, D. J.,
1007 Bey, I., Bian, H., Cuvelier, C., Duncan, B. N., Folberth, G., Horowitz, L. W., Jonson, J., Kaminski, J. W., Marmer, E.,
1008 Park, R., Pringle, K. J., Schroeder, S., Szopa, S., Takemura, T., Zeng, G., Keating, T. J., and Zuber, A.: A multi-model
1009 assessment of pollution transport to the Arctic, *Atmos. Chem. Phys.*, 8, 5353-5372, 10.5194/acp-8-5353-2008, 2008.

1010 Sigl, M., McConnell, J. R., Layman, L., Maselli, O., McGwire, K., Pasteris, D., Dahl-Jensen, D., Steffensen, J. P., Vinther,
1011 B., Edwards, R., Mulvaney, R., and Kipfstuhl, S.: A new bipolar ice core record of volcanism from WAIS Divide and
1012 NEEM and implications for climate forcing of the last 2000 years, *J. Geophys. Res.-Atmos.*, 118, 1151-1169,
1013 10.1029/2012jd018603, 2013.

1014 Simoneit, B. R. T., Schauer, J. J., Nolte, C. G., Oros, D. R., Elias, V. O., Fraser, M. P., Rogge, W. F., and Cass, G. R.:
1015 Levoglucosan, a tracer for cellulose in biomass burning and atmospheric particles, *Atmos. Environ.*, 33, 173-182, 1999.

1016 Simoneit, B. R. T.: Biomass burning - A review of organic tracers for smoke from incomplete combustion, *Appl. Geochem.*,
1017 17, 129-162, 2002.

1018 Sorrel, P., Oberhansli, H., Boroffka, N., Nourgaliev, D., Dulski, P., and Rohl, U.: Control of wind strength and frequency in
1019 the Aral Sea basin during the late Holocene, *Quat. Res.*, 67, 371-382, 10.1016/j.yqres.2006.12.003, 2007.

1020 St. George, S. S., Meko, D. M., Girardin, M. P., MacDonald, G. M., Nielsen, E., Pederson, G. T., Sauchyn, D. J., Tardif, J.
1021 C., and Watson, E.: The Tree-Ring Record of Drought on the Canadian Prairies, *J. Clim.*, 22, 689-710,
1022 10.1175/2008jcli2441.1, 2009.

1023 Stahle, D. W., Cook, E. R., Cleaveland, M. K., Therrell, M. D., Meko, D. M., Grissino-Mayer, H. D., Watson, E., and
1024 Luckman, B. H.: Tree-ring data document 16th century megadrought over North America, *Eos, Transactions American*
1025 *Geophysical Union*, 81, 121-125, 10.1029/00eo00076, 2000.

1026 Stohl, A.: Characteristics of atmospheric transport into the Arctic troposphere, *J. Geophys. Res.-Atmos.*, 111,
1027 10.1029/2005jd006888, 2006.

1028 Stohl, A., Andrews, E., Burkhart, J. F., Forster, C., Herber, A., Hoch, S. W., Kowal, D., Lunder, C., Mefford, T., Ogren, J.
1029 A., Sharma, S., Spichtinger, N., Stebel, K., Stone, R., Strom, J., Torseth, K., Wehrli, C., and Yttri, K. E.: Pan-Arctic
1030 enhancements of light absorbing aerosol concentrations due to North American boreal forest fires during summer 2004,
1031 *J. Geophys. Res.-Atmos.*, 111, 10.1029/2006jd007216, 2006.

1032 Tan, M., Liu, T. S., Hou, J. Z., Qin, X. G., Zhang, H. C., and Li, T. Y.: Cyclic rapid warming on centennial-scale revealed
1033 by a 2650-year stalagmite record of warm season temperature, *Geophys. Res. Lett.*, 30, 1617, 10.1029/2003gl017352,
1034 2003.

1035 Taylor, K. C., Mayewski, P. A., Twickler, M. S., and Whitlow, S. I.: Biomass burning recorded in the GISP2 ice core: A
1036 record from eastern Canada?, *Holocene*, 6, 1-6, 1996.

1037 The Milwaukee Journal: Alaska, Russia battle blazes, Milwaukee, Wisconsin, Aug. 09 1972.

1038 The New York Times: Smoke shrouds Moscow as peat-bog fire rages, Aug. 09 1972, New York.

1039 The Palm Beach Post: Thousands fight Russia Peat fire, Aug. 09 1972.

1040 Thompson, L. G., Yao, T., Mosley-Thompson, E., Davis, M. E., Henderson, K. A., and Lin, P. N.: A high-resolution
1041 millennial record of the South Asian Monsoon from Himalayan ice cores, *Science*, 289, 1916-1919,
1042 10.1126/science.289.5486.1916, 2000.

1043 Trentmann, J., Luderer, G., Winterrath, T., Fromm, M. D., Servranckx, R., Textor, C., Herzog, M., Graf, H. F., and
1044 Andreae, M. O.: Modeling of biomass smoke injection into the lower stratosphere by a large forest fire (Part I):
1045 reference simulation, *Atmos. Chem. Phys.*, 6, 5247-5260, 2006.

1046 Turquety, S., Logan, J. A., Jacob, D. J., Hudman, R. C., Leung, F. Y., Heald, C. L., Yantosca, R. M., Wu, S. L., Emmons, L.
1047 K., Edwards, D. P., and Sachse, G. W.: Inventory of boreal fire emissions for North America in 2004: Importance of
1048 peat burning and pyroconvective injection, *J. Geophys. Res.-Atmos.*, 112, 10.1029/2006jd007281, 2007.

1049 van der Werf, G. R., Randerson, J. T., Collatz, G. J., Giglio, L., Kasibhatla, P. S., Arellano, A. F., Olsen, S. C., and
1050 Kasichke, E. S.: Continental-scale partitioning of fire emissions during the 1997 to 2001 El Nino/La Nina period,
1051 *Science*, 303, 73-76, 10.1126/science.1090753, 2004.

1052 van der Werf, G. R., Peters, W., van Leeuwen, T. T., and Giglio, L.: What could have caused pre-industrial biomass burning
1053 emissions to exceed current rates?, *Clim. Past*, 9, 289-306, 10.5194/cp-9-289-2013, 2013.

1054 van Mantgem, P. J., Stephenson, N. L., Byrne, J. C., Daniels, L. D., Franklin, J. F., Fule, P. Z., Harmon, M. E., Larson, A.
1055 J., Smith, J. M., Taylor, A. H., and Veblen, T. T.: Widespread Increase of Tree Mortality Rates in the Western United
1056 States, *Science*, 323, 521-524, 10.1126/science.1165000, 2009.

1057 Vinther, B. M., Clausen, H. B., Johnsen, S. J., Rasmussen, S. O., Andersen, K. K., Buchardt, S. L., Dahl-Jensen, D.,
1058 Seierstad, I. K., Siggaard-Andersen, M. L., Steffensen, J. P., Svensson, A., Olsen, J., and Heinemeier, J.: A synchronized
1059 dating of three Greenland ice cores throughout the Holocene, *J. Geophys. Res.-Atmos.*, 111, D13102,
1060 10.1029/2005jd006921, 2006.

1061 Wang, Z., Chappellaz, J., Park, K., and Mak, J. E.: Large Variations in Southern Hemisphere Biomass Burning During the
1062 Last 650 Years, *Science*, 330, 1663-1666, 10.1126/science.1197257, 2010.

1063 Wang, Z.-h., Chen, Z.-y., Kou, Y., and Chen, Y.: Dry/Wet climate change since 960 A. D. in taihu drainage basin of China,
1064 *Chin. Geograph.Sc.*, 11, 343-349, 10.1007/s11769-001-0050-0, 2001.

1065 Wanner, H., Beer, J., Butikofer, J., Crowley, T. J., Cubasch, U., Fluckiger, J., Goosse, H., Grosjean, M., Joos, F., Kaplan, J.
1066 O., Kuttel, M., Muller, S. A., Prentice, I. C., Solomina, O., Stocker, T. F., Tarasov, P., Wagner, M., and Widmann, M.:

1067 Mid- to Late Holocene climate change: an overview, *Quat. Sci. Rev.*, 27, 1791-1828, 10.1016/j.quascirev.2008.06.013,
1068 2008.

1069 Ward, D. S., Kloster, S., Mahowald, N. M., Rogers, B. M., Randerson, J. T., and Hess, P. G.: The changing radiative forcing
1070 of fires: global model estimates for past, present and future, *Atmos. Chem. Phys.*, 12, 10857-10886, 10.5194/acp-12-
1071 10857-2012, 2012.

1072 Weimer, S., Alfarra, M. R., Schreiber, D., Mohr, M., Prévôt, A. S. H., and Baltensperger, U.: Organic aerosol mass spectral
1073 signatures from wood-burning emissions: Influence of burning conditions and wood type, *Journal of Geophysical
1074 Research: Atmospheres*, 113, D10304, 10.1029/2007jd009309, 2008.

1075 Weng, H. Y.: Impacts of multi-scale solar activity on climate. Part I: Atmospheric circulation patterns and climate extremes,
1076 *Adv. Atmos. Sci.*, 29, 867-886, 10.1007/s00376-012-1238-1, 2012.

1077 Westerling, A. L., Hidalgo, H. G., Cayan, D. R., and Swetnam, T. W.: Warming and earlier spring increase western US
1078 forest wildfire activity, *Science*, 313, 940-943, 10.1126/science.1128834, 2006.

1079 Whitlow, S., Mayewski, P., Dibb, J., Holdsworth, G., and Twickler, M.: An ice-core-based record of biomass burning in the
1080 arctic and sub-arctic, 1750-1980, *Tellus Ser. B-Chem. Phys. Meteorol.*, 46, 234-242, 1994.

1081 Wolfe, S. A., Huntley, D. J., David, P. P., Ollerhead, J., Sauchyn, D. J., and MacDonald, G. M.: Late 18th century drought-
1082 induced sand dune activity, Great Sand Hills, Saskatchewan, *Can. J. Earth Sci.*, 38, 105-117, 10.1139/cjes-38-1-105,
1083 2001.

1084 Wolff, E. W., Barbante, C., Becagli, S., Bigler, M., Boutron, C. F., Castellano, E., de Angelis, M., Federer, U., Fischer, H.,
1085 Fundel, F., Hansson, M., Hutterli, M., Jonsell, U., Karlin, T., Kaufmann, P., Lambert, F., Littot, G. C., Mulvaney, R.,
1086 Rothlisberger, R., Ruth, U., Severi, M., Siggaard-Andersen, M. L., Sime, L. C., Steffensen, J. P., Stocker, T. F.,
1087 Traversi, R., Twarloh, B., Udisti, R., Wagenbach, D., and Wegner, A.: Changes in environment over the last 800,000
1088 years from chemical analysis of the EPICA Dome C ice core, *Quat. Sci. Rev.*, 29, 285-295,
1089 10.1016/j.quascirev.2009.06.013, 2010a.

1090 Wolff, E. W., Chappellaz, J., Blunier, T., Rasmussen, S. O., and Svensson, A.: Millennial-scale variability during the last
1091 glacial: The ice core record, *Quat. Sci. Rev.*, 29, 2828-2838, 10.1016/j.quascirev.2009.10.013, 2010b.

1092 Wolken, J. M., Hollingsworth, T. N., Rupp, T. S., Chapin, F. S., Trainor, S. F., Barrett, T. M., Sullivan, P. F., McGuire, A.
1093 D., Euskirchen, E. S., Hennon, P. E., Beever, E. A., Conn, J. S., Crone, L. K., D'Amore, D. V., Fresco, N., Hanley, T.
1094 A., Kielland, K., Kruse, J. J., Patterson, T., Schuur, E. A. G., Verbyla, D. L., and Yarie, J.: Evidence and implications of
1095 recent and projected climate change in Alaska's forest ecosystems, *Ecosphere*, 2, art124, 10.1890/es11-00288.1, 2011.

1096 Wooster, M. J., and Zhang, Y. H.: Boreal forest fires burn less intensely in Russia than in North America, *Geophys. Res.
1097 Lett.*, 31, 10.1029/2004gl020805, 2004.

1098 Yalcin, K., Wake, C. R., Kreutz, K. J., and Whitlow, S. I.: A 1000-yr record of forest fire activity from Eclipse Icefield,
1099 Yukon, Canada, Holocene, 16, 200-209, 10.1191/0959683606hl920rp, 2006.

1100 Yang, B., Braeuning, A., Johnson, K. R., and Shi, Y. F.: General characteristics of temperature variation in China during the
1101 last two millennia, *Geophys. Res. Lett.*, 29, 1324, 10.1029/2001gl014485, 2002.

1102 Yang, B., Brauning, A., Zhang, Z., Dong, Z., and Esper, J.: Dust storm frequency and its relation to climate changes in
1103 Northern China during the past 1000 years, *Atmos. Environ.*, 41, 9288-9299, 10.1016/j.atmosenv.2007.09.025, 2007.

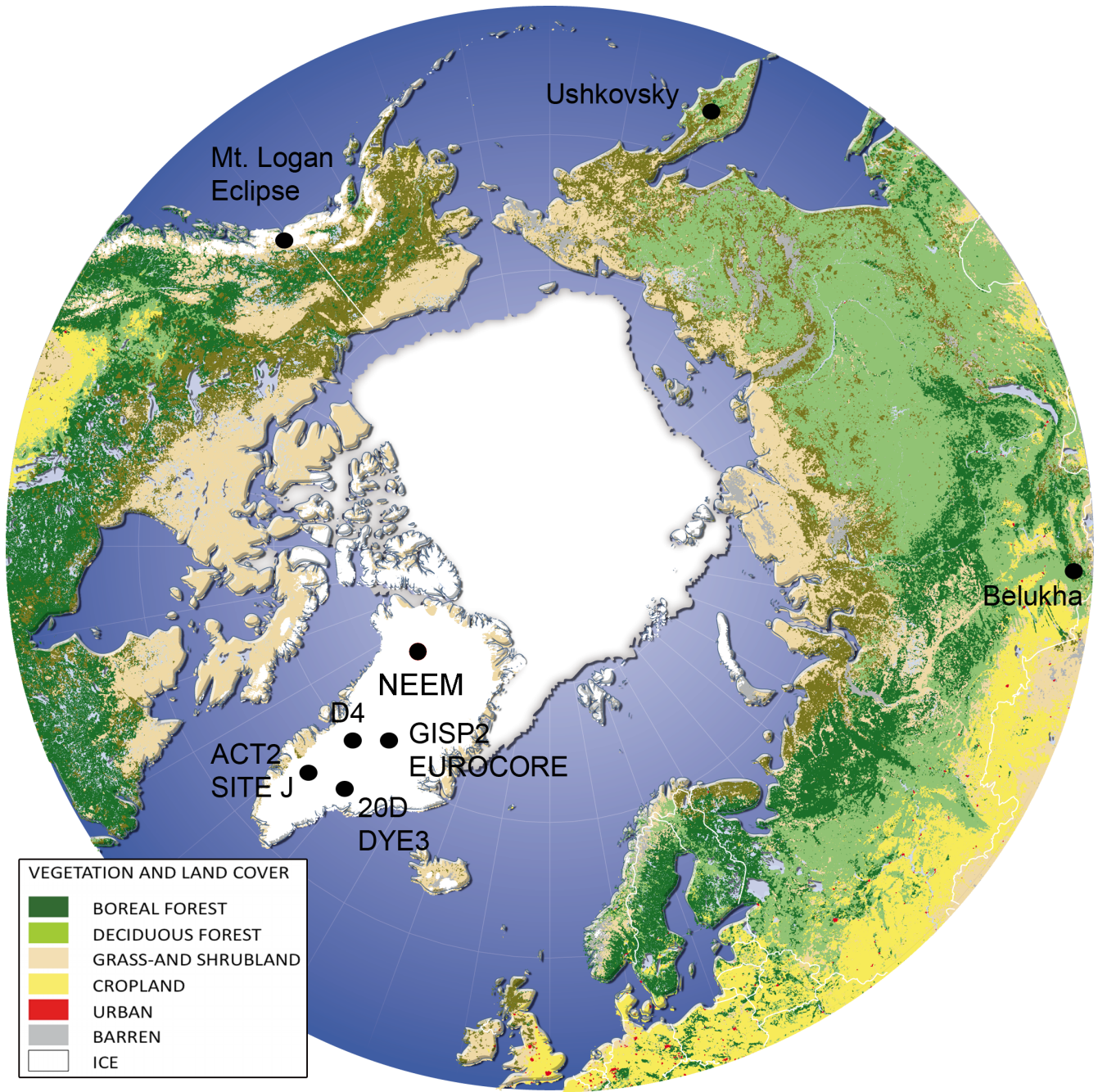
1104 Yao, P., Schwab, V. F., Roth, V., Xu, B., Yao, T., and Gleixner, G.: Levoglucosan concentrations in ice-core samples from
1105 the Tibetan Plateau determined by reverse-phase high-performance liquid chromatography-mass spectrometry, *J.
1106 Glaciol.*, 59, 599-608, 2013.

1107 Zhang, P. Z., Cheng, H., Edwards, R. L., Chen, F. H., Wang, Y. J., Yang, X. L., Liu, J., Tan, M., Wang, X. F., Liu, J. H.,
1108 An, C. L., Dai, Z. B., Zhou, J., Zhang, D. Z., Jia, J. H., Jin, L. Y., and Johnson, K. R.: A Test of Climate, Sun, and
1109 Culture Relationships from an 1810-Year Chinese Cave Record, *Science*, 322, 940-942, 10.1126/science.1163965, 2008.

1110 Zhang, Y. H., Wooster, M. J., Tutubalina, O., and Perry, G. L. W.: Monthly burned area and forest fire carbon emission
1111 estimates for the Russian Federation from SPOT VGT, *Remote Sens. Environ.*, 87, 1-15, 10.1016/s0034-
1112 4257(03)00141-x, 2003.

1113

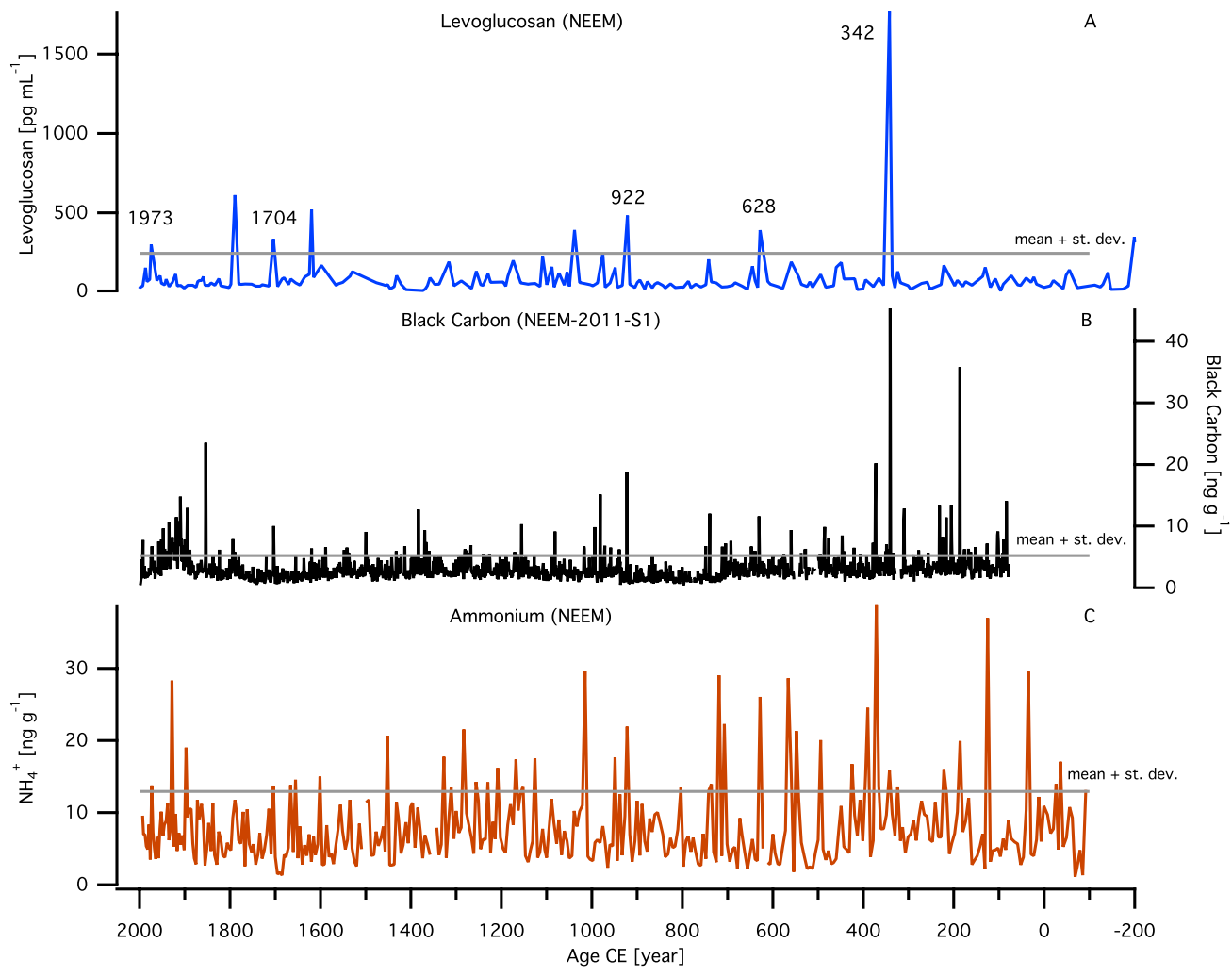
1114



1118 **Fig. 1.** NEEM camp position and representation of boreal vegetation and land cover between 50° and 90° N.

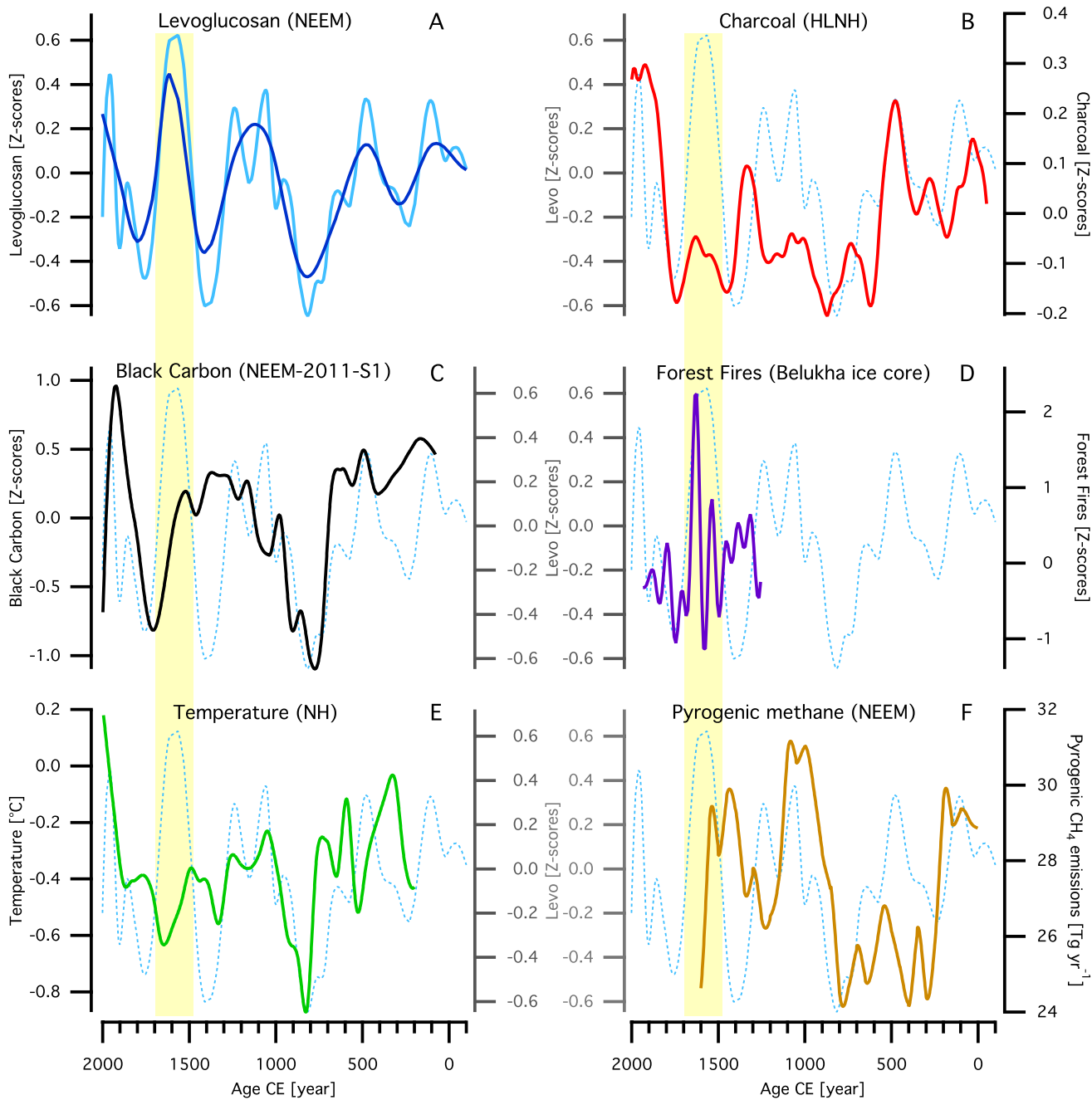
1119 Modified from the European Commission Global Land Cover 2000 database and based on the work of

1120 cartographer Hugo Alhenius UNEP/GRIP-Arendal (Alhenius, 2003).



1122
 1123
 1124
 1125
 1126
 1127

Fig. 2. A: Levoglucosan concentration profile measured in the deep NEEM core including the dates of megafires coincident between levoglucosan, black carbon, and ammonium; B: black carbon concentration profile measured in the NEEM-2011-S1 ice core; C: ammonium concentration profile in the deep NEEM ice core.



1128

1129

1130

1131

1132

1133

1134

Fig. 3. LOWESS smoothing with SPAN parameter (f) 0.1 (light blue) and 0.2 (dark blue) of levoglucosan Z-scores without peaks above the threshold $3rd_Q + 1.5 \times IR$ (A); High Latitude (above $55^\circ N$) Northern Hemisphere (HLNH) Z-scores of charcoal influx (200-yr LOWESS smoothing) as reported in Marlon *et al.* (2008) (red) and smoothed levoglucosan with $f = 0.1$ as in A (dashed line) (B); LOWESS smoothing with $f = 0.1$ of Black Carbon Z-scores without peaks above the threshold $3rd_Q + 1.5 \times IR$ (black) and smoothed levoglucosan (dashed line)(C); Siberian forest fire reconstruction (Eichler *et al.*, 2011) (purple) and smoothed

1135 levoglucosan (dashed line) (D); LOWESS smoothing with $f = 0.1$ of Northern Hemisphere land temperature
1136 (Mann et al., 2008) and smoothed levoglucosan (dashed line) (E); pyrogenic CH₄ emissions inferred from the
1137 deep NEEM core (Sapart et al., 2012) (light brown) and smoothed levoglucosan (dashed line) (F). The yellow
1138 vertical bar indicates the period of strongest fire activity.
1139

LEVOGLUCOSAN						BLACK CARBON			AMMONIUM	
Sample Age (yr CE)	Average age (yr CE)	[levoglucosan] (pg mL ⁻¹)	Z-score ¹	Z-score ²	Age (yr CE)	[BC] (ng g ⁻¹)	Z-score ²	[NH ₄ ⁺] (ng g ⁻¹)	Z-score ²	
1975	1972	1973	301	1.37	1.45	1972.5	6.73	1.68	13.77	1.16
1791	1787	1789	612	3.39	3.56	1789.5	5.81	1.26		
1706	1702	1704	336	1.59	1.69	1703.5	10.02	3.15	13.75	1.16
						1702.5	5.85	1.28		
1622	1617	1620	521	2.80	2.94	1619.5	6.35	1.51		
1603 ³	1593 ³	1598 ³	170 ³	0.51 ³	0.55 ³	1594.5	5.29	1.03	14.98 ³	1.39 ³
1319	1313	1316	193	0.66	0.71					
1177	1171	1174	201	0.71	0.77	1170.5	5.80	1.26		
1112	1106	1109	229	0.90	0.96					
1041	1036	1039	393	1.96	2.07					
979	973	976	245	1.00	1.06	974.5	5.38	1.07		
924	919	922	483	2.55	2.69	922.5	18.85	7.11	21.93	2.71
745	739	742	208	0.76	0.81	739.5	12.02	4.05	13.01	1.02
631	625	628	391	1.95	2.06	630.5	11.58	3.85	26.07	3.50
562	556	559	192	0.65	0.70	559.5	9.35	2.85	15.07	1.41
451	446	449	188	0.63	0.68	446.5	8.47	2.46		
345	339	342	1767	10.92	11.42	345.5	6.26	1.46	15.83	1.55
						340.5	45.32	18.98		
225	219	222	170	0.51	0.56	224.5	8.23	2.35	16.02	1.59
						223.5	7.22	1.90		
						221.5	6.69	1.66		
-196	-202	-199	349	1.68	1.78	<i>na</i>	<i>na</i>	<i>na</i>	26.44	3.57
-271	-277	-274	401	2.02	2.13	<i>na</i>	<i>na</i>	<i>na</i>	22.08	2.74
-327	-333	-330	382	1.89	2.00	<i>na</i>	<i>na</i>	<i>na</i>		
-389	-396	-392	1445	8.82	9.23	<i>na</i>	<i>na</i>	<i>na</i>		
-524	-531	-527	192	0.65	0.70	<i>na</i>	<i>na</i>	<i>na</i>	21.56	2.64
-537	-543	-540	266	1.14	1.21	<i>na</i>	<i>na</i>	<i>na</i>	12.97	1.01
-584	-590	-587	185	0.61	0.66	<i>na</i>	<i>na</i>	<i>na</i>		

1140

1141 **Table 1.** Major levoglucosan peaks (with levoglucosan concentrations above the threshold 3rd Q + 1.5 IR) and
1142 their correspondence with other biomass burning proxies. Samples in bold have levoglucosan concentrations
1143 above the mean plus one standard deviation. The NH₄⁺ samples have the same ages as the levoglucosan samples.
1144 Blank spaces demonstrate the absence of high values (Z-scores > 1), *na* if no values were available.

1145 ¹ Mean and standard deviation calculated for the entire levoglucosan dataset (1036 BCE - 1999 CE).

1146 ² Mean and standard deviation calculated for the common period (87 - 1992 CE) of the BC, levoglucosan and
 1147 ammonium dataset in order to compare datasets covering different temporal periods.

1148 ³ Levoglucosan has been analyzed in a 4-bag sample (1593 - 1603 CE); ammonium value is referred to a 2-bag
 1149 sample (1598 - 1603 CE).

1150

AGE ^a	LOCATION	PROXY	REFERENCE	COMMENT
1171-1177	NEEM ice core	levoglucosan	this work	strong event¹
1170	Taihu Drainage Basin China, Eastern Cost	historical climatic records	(Wang et al., 2001)	abrupt dry/wet climate change
1160-1290	Northern China (reconstruction based on different paleoclimate archives)	flood/drought index	(Yang et al., 2007) and ref. therein	max frequency of dust storm
1313-1319	NEEM ice core	levoglucosan	this work	strong event¹
1320-1370	Northern China (reconstruction based on different paleoclimate archives)	flood/drought index	(Yang et al., 2007) and ref. therein	high dust fall frequency
1330s	Dasuopu ice core, Himalaya (India and Asia as source regions)	$\delta^{18}\text{O}$, dust, Cl^-	(Thompson et al., 2000)	monsoon failure
1593-1603	NEEM ice core	levoglucosan	this work	strong event¹
1617-1622	NEEM ice core	levoglucosan	this work	megaevent²
1578-1582 1600-1644	Mongolia	tree-ring	(Davi et al., 2010)	2 nd and 1 st in order of severity since 1520
1590s-1600s	Central High Asia	tree-ring	(Fang et al., 2010)	
1590s	Dasuopu ice core, Himalaya (India and Asia as source regions)	$\delta^{18}\text{O}$, dust, Cl^-	(Thompson et al., 2000)	monsoon failure
exceptional events: 1586-1589; 1638-1641 decadal time scale: 1590s	Eastern China	drought/flood proxy data	(Shen et al., 2007)	most severe events (exceptional) of past 5 centuries
1618-1635	Taihu Drainage Basin China, Eastern Cost	historical climatic records	(Wang et al., 2001)	abrupt change to dry period
1702-1706	NEEM ice core	levoglucosan	this work	megaevent²
1694-1705	Changling Mountains, North-central China	tree-ring	(Feng et al., 2011)	coincident with Maunder Minimum ³
1787-1791	NEEM ice core	levoglucosan	this work	megaevent²
1795-1823	Changling Mountains, north-central China	tree-ring	(Chen et al., 2012)	coincides with Dalton Minimum ³
1790-1799	North Helan Mountain, inner Mongolia	tree-ring	(Liu et al., 2004)	
1791-1795	Northeastern Mongolia	tree-ring	(Pederson et al., 2001)	
1779-1806	Chiefeng-Weichang region, China	tree-ring	(Liu et al., 2010)	
1790-1796	Dasuopu ice core, Himalaya (India and Asia as source regions)	$\delta^{18}\text{O}$, dust, Cl^-	(Thompson et al., 2000)	monsoon failures “exceptionally large from a perspective of the last 1000 yr”
1789-1793	India	archival evidences of drought	(Grove, 1998)	

PERIOD^b	LOCATION	PROXY	REFERENCE	COMMENT
1500 - 1700	NEEM ice core	levoglucosan	this work	multi-decadal analysis
centennial scale: 16 th , 17 th century	Eastern China	drought/flood proxy data	(Shen et al., 2007)	
1610-1710	Northern China (reconstruction based on different paleoclimate archives)	flood/drought index	(Yang et al., 2007) and references therein	high dust fall frequency
1540-1600	Siberian Altai (Southern Siberia)	ice core pollen data and dust	(Eichler et al., 2011)	extremely dry period followed by high fire activity
1414-1560	Lake Teletskoye, Republic of Altai (Russian Federation)	sediment core pollen data	(Andreev et al., 2007)	
1450-1600	Eastern China	historical documents	(Chu et al., 2008)	negative snow anomaly events
1400-1550	East Juyanhai Lake Inner Mongolia	sedimentology and geochemical parameters	(Chen et al., 2010)	extremely arid conditions
1630s-1640s	Xiaolong Mountain, central China	tree-ring	(Fang et al., 2012)	one of most severe droughts of the past 400 yr
1630s-1640s	China and Mongolia	tree-ring	(Li et al., 2009)	
1640s	Dasuopu ice core, Himalaya (India and Asia as source regions)	$\delta^{18}\text{O}$, dust, Cl^-	(Thompson et al., 2000)	monsoon failure
1640s-1650s	Central High Asia	tree-ring	(Fang et al., 2010)	most severe megadrought

1151

1152 **Table 2.** Asian droughts recorded in various proxies with strong fire events (a) and with centennial fire activity
1153 in the 16th and 17th century inferred from levoglucosan analysis (b). Generally drought is recorded in tree-rings
1154 as a sustained narrowness of growth rings.

1155 ¹ This event represents levoglucosan concentration above the threshold $3^{\text{rd}} \text{ Q} + 1.5 \text{ IR}$. Where 3^{rd} Q is the third
1156 quartile and IR is the interquartile range calculates as the difference between the third quartile and the first
1157 quartile. This peak was removed from the long-trend analysis.

1158 ² This event represents levoglucosan concentration above the mean plus one standard deviation.

1159 ³ As noted by Chen (2012), the drying of the late 1600s to early 1700s, and the drying of the late 1700s to early
1160 1800s, seen in the precipitation reconstructions, coincides with periods of low solar irradiance, the Dalton
1161 Minimum and the Maunder Minimum, respectively.